

# The evolution of the $V - K$ colours of single stellar populations

Léo Girardi<sup>1,2</sup> and Gianpaolo Bertelli<sup>3,4</sup>

<sup>1</sup>*Max-Planck-Institut für Astrophysik, Karl-Schwarzschild-Str. 1, D-87540 Garching bei München, Germany*

<sup>2</sup>*Alexander von Humboldt fellow*

<sup>3</sup>*National Council of Research (CNR-GNA)*

<sup>4</sup>*Department of Astronomy, Padova University, Vicolo dell'Osservatorio 5, I-35122 Padova, Italy*

Accepted 19?? ???. Received 1997 ???; in original form 1997 ???

## ABSTRACT

Models of evolutionary population synthesis of galaxies rely on the properties of the so-called single stellar populations (SSP). In this paper, we discuss how the integrated near-infrared colours – and especially  $V - K$  – of SSPs evolve with age and metallicity. Some of the uncertainties associated to the properties of the underlying stellar models are throughfully discussed.

Our models include all the relevant stellar evolutionary phases, with particular attention being dedicated to the AGB, which plays a fundamental role in the evolution of the near-infrared part of the spectrum. First, we present the effects that different formulations for the mass-loss rates produce on the final remnant mass (i.e., on the initial–final mass relation), and hence on the AGB-termination luminosity and the relative contribution of these stars to the integrated light. The results for the evolution of the  $V - K$  colour are very different depending on the choice of the mass-loss prescription; the same happens also for the  $B - V$  colour in the case of low-metallicity SSPs. Second, we describe the changes occurring in the integrated colors at the onset of the AGB and RGB stars. According to the classical formalism for the AGB evolution, the onset of this evolutionary phase is marked by a color jump to the red, whose amplitude is shown here to be highly dependent on the metallicity and mass-loss rates adopted in the models. We then consider the effect of the overluminosity with respect to the standard core mass-luminosity relation, that occurs in the most massive AGB stars. Different simplified formulations for this effect are tested in the models; they cause a smoothing of the colour evolution in the age range at which the AGB starts to develop, rather than a splitting of the color jump into two separate events. On the other hand, we find that a temporary red phase takes place  $\sim 1.5 \times 10^8$  yr after the RGB develops. Thanks to the transient nature of this feature, the onset of the RGB is probably not able to cause marked features in the spectral evolution of galaxies.

We then discuss the possible reasons for the transition of  $V - K$  colours (from  $\sim 1.5$  to 3) that takes place in LMC clusters of SWB type IV (Persson et al. 1983). A revision of the ages attributed to the single clusters reveals that the transition may not be as fast as originally suggested. The comparison of the data with the models indicates that it results mainly from the development of the AGB. A gradual (or delayed) transition of the colours, as predicted by models which include the overluminosity of the most massive AGB stars, seems to describe better the data than the sudden colour-jump predicted by classical models.

**Key words:** stars: evolution – stars: AGB – stars: mass loss – infrared: general – galaxies: star clusters – Magellanic Clouds

## 1 INTRODUCTION

Models of evolutionary population synthesis are nowadays an important tool for the study of nearby and distant galax-

ies. In them, the spectral features observed in the integrated light of galaxies are synthesized by summing the theoretical spectra of single stellar populations (hereafter SSPs), as a way to get information into the galactic history of stellar for-

mation and chemical enrichment (e.g. Tinsley 1980; Bruzual & Charlot 1993; Bressan, Chiosi & Fagotto 1994b; Worthey 1994; Weiss, Peletier & Matteucci 1995).

SSPs are defined as representative ensembles of stars of single age and metallicity. They can be constructed by interpolation on extended grids of stellar evolutionary tracks and spectra, and under the usual assumption that the mass distribution of the stars is given by a known initial mass function. The reliability of the SSP properties as a function of their two fundamental parameters – age and metallicity – is secured by the previous testing of the stellar tracks and derived isochrones against observations of stars in the solar neighbourhood and in star clusters. Moreover, SSP models can be independently tested by comparing their spectral properties with those observed in *real* single-burst stellar populations. The best known examples of these objects are star clusters, for which the internal spread of stellar ages and metallicities is generally small enough to be neglected.

The comparison between the properties of SSPs and star clusters has been performed by several authors, mostly with relation to the integrated broad-band colours (e.g. Chiosi, Bertelli & Bressan 1988; Arimoto & Bica 1989; Battinelli & Capuzzo-Dolcetta 1989; Barbaro & Olivi 1991; Girardi & Bica 1993). This is a first step preliminary to comparing spectral features. In a previous work (Girardi et al. 1995), we showed that a particular set of models – namely those from the Padova group (see Bressan et al. 1994b; Bertelli et al. 1994) – reproduces quite well two basic observational relations for the visual colours, namely:

1) *The linear relation between the  $S$  parameter in the  $(U - B)$  vs.  $(B - V)$  diagram and the logarithm of the age, found in the star clusters of the Magellanic Clouds by Elson & Fall (1985). SSP models with near-solar metallicity\* reproduce this linear behaviour to a high extent, over most of the age interval that comprehends young and intermediate-age star clusters.*

2) *The sequence of colours of galactic globular clusters by Racine (1973). The models for old SSPs (with  $\sim 15$  Gyr) are able to reproduce both the slope and metallicity dependence of this sequence in the  $(U - B)$  vs.  $(B - V)$  plane. There are however, small systematic shifts [of  $\Delta(B - V) = 0.05$  and  $\Delta(U - B) = -0.03$  mag] between the Padova models and the observations, which can be attributed mostly to small inadequacies in the  $T_{\text{eff}}$ -colour transformations from Kurucz (1992; see also Charlot, Worthey & Bressan 1996).*

This success in reproducing the observational relations is not an exclusivity of the Padova models: similar behaviours for the  $UBV$  colours can be found in several of the evolutionary population synthesis models available in the literature. This is so because these colours – for both young and intermediate-age SSPs of near-solar metallicity, and for old SSPs of low-metallicity, – are mainly determined by the stars in the well-understood evolutionary stage of main sequence (MS). These stars are known to evolve in a regular

way in the HR diagram, as a function of both age and metallicity. The stars in the stage of core He-burning (CHeB) have a secondary importance in determining the visual colours of SSPs. Although several uncertainties persist in the theoretical predictions for this evolutionary phase – about e.g. the role of different convective phenomena as core overshooting, semiconvection, and breathing pulses (see Chiosi, Bertelli & Bressan 1992) –, its behaviour in the HR diagram is also reasonably regular. Moreover, its contribution to the integrated colours is generally overwhelmed by that of the main sequence. Thus, the CHeB stars are not able to change much the colour behaviour dictated by the main sequence stars. These considerations are not valid for the very young SSPs of near-solar metallicity, since for high-mass stars the evolution of the CHeB phase in the HR diagram can significantly change with age and metallicity, and as a function of the selected scheme of internal mixing. Higher uncertainties in the predicted visual colours result in this case (cf. Girardi & Bica 1993).

Near-infrared colours behave quite differently from the regular trends found in the evolution of visual colours. They are practically determined by the evolution of the stars of later evolutionary phases, especially those in the red and asymptotic giant branches (RGB and AGB respectively), and by the red supergiants in the case of the youngest SSPs. This leads to a non-regular evolution of the colours with age and metallicity, since the amount and position of these stars in the HR diagram is known to vary as a function of both parameters – and most remarkably as a function of age.

Let us focus our analysis on those stellar populations which contain RGB and AGB stars. Stellar models predict that, as we go from higher to lower stellar initial masses, these evolutionary phases appear rather suddenly when we reach the upper mass limits for the development of degenerate carbon-oxygen and helium cores,  $M_{\text{up}}$  and  $M_{\text{HeF}}$ , respectively. The presence of these well-defined transition masses then translate into major changes on the HR diagram properties of star clusters over relatively small time scales. Renzini & Buzzoni (1986) concluded that the development of both AGB and RGB should be accompanied by sudden jumps of the SSPs to redder integrated colors, events which they called ‘phase transitions’. The concept of phase transitions became very popular because they seemed to furnish a plausible explanation for the bimodal distribution of the integrated  $B - V$  colors of LMC clusters (see van den Bergh 1981), and because they could provide useful ‘evolutionary clocks’ for age-dating galaxies at large redshifts (cf. Renzini & Buzzoni 1986). However, Chiosi et al. (1988) first concluded, with the aid of complete models of SSPs, that the developments of the RGB is not accompanied by a noticeable jump in the  $B - V$  colors, and that the bimodality in the distribution of colors of LMC clusters could be attributed to other causes. The latter conclusion was corroborated by the recent analysis of Girardi et al. (1995). On the other hand, the colour jump due to the development of the AGB was shown to be negligible in visual colours, and was predicted to occur at too young ages to be useful in the age-dating of distant galaxies (Bressan et al. 1994b).

However, the interest on the phase transition events has been renewed by the suggestion of Renzini (1992) that the colour jump due to the AGB phase transition could be severely delayed due to the effect of envelope burning

\* In this paper we use the term ‘near-solar metallicity’ in opposition to ‘low-metallicity’, which is usually attributed to the globular clusters of the galactic halo. For the sake of clarity, let us consider  $Z = 0.008$  (the metallicity of the young populations in the Large Magellanic Cloud) as being the limit between low and near-solar metallicity.

that occurs in the most massive AGB stars (Blöcker & Schönberner 1991). In this case, the AGB phase transition could again be considered as a candidate for being a useful evolutionary clock. Moreover, since the effects of the AGB and RGB development should be expected to be stronger in the near-infrared colours, they were suggested to be at the origin of the apparently rapid transition in  $V - K$  colours, from  $\sim 1.5$  to 3, which occurs in the LMC clusters of SWB type IV (see Renzini 1992; Corsi et al. 1994). In fact, the origin of this colour change remains to be properly explained in the context of SSP models.

In this paper, we readdress the expected behaviour of the integrated colours for those stellar populations that do contain AGB stars, with the aim of casting light on the above mentioned points. Although our main target is the study of the evolution of near-infrared colours – mainly  $V - K$  –, we will also present the results for the  $B - V$  colour for the sake of comparison. In Section 2 we present an overview of the methods used to calculate integrated colours of SSPs, briefly considering what is the expected behaviour of the near-IR colours, with base in the fuel consumption theorem by Renzini & Buzzoni (1986). Then we present the grid of stellar evolutionary tracks which we use in order to calculate theoretical isochrones. They include all evolutionary phases from the main sequence to the end of the early (E-) AGB. The thermally pulsing (TP-) AGB is included by means of a synthetic model. Some of the uncertainties, related to the mass-loss rates and to the presence of ‘overluminous’ AGB stars with envelope burning, are thoroughly discussed. In Section 3 we present the colour evolution based on the isochrone method, discuss how it depends on several factors, and revise the features that arise in the colours when the AGB and RGB develop. Section 4 is dedicated to the study of the near-infrared colours ( $V - K$ ,  $J - K$ , and  $H - K$ ) observed in Magellanic Cloud star clusters. The results are briefly commented in Section 5.

## 2 THEORETICAL BACKGROUND AND STELLAR MODELS

### 2.1 The isochrone method and the fuel consumption theorem

The simplest representation of single stellar populations is provided by isochrones of given age and metallicity. These are produced from stellar evolutionary tracks by means of a simple transformation from the time evolution of stellar properties for several initial masses  $[f(t)_{M_i}]$ , to the mass sequence of those properties for several ages  $[f(M_i)_t]$ . The reliability of this kind of transformation is secured by a fit mass grid of stellar tracks and a suitable interpolation algorithm.

Once we have a set of isochrones, integrated colours of ideal SSPs can be obtained by simply summing the contribution of different stars, corresponding to different stellar masses, to the total light in a given pass-band  $\lambda$  (see e.g. Alongi & Chiosi 1989; Girardi & Bica 1993; Charlot & Bruzual 1991). For a given SSPs of age  $t$  we have

$$L_{\lambda}^{\text{SSP}}(t) = \int_0^{\infty} \phi_M L_{\lambda M}(t) dM \quad (1)$$

where  $L_{\lambda M}(t)$  corresponds to the luminosity along the isochrone, and  $\phi_M$  is the initial mass function. The IMF is usually normalized so that the total SSP mass is equal to a known quantity  $M_T$ , i.e.

$$\int_0^{\infty} M \phi_M dM = M_T.$$

Integrated magnitudes and colours follow straightforwardly from the quantities  $L_{\lambda}^{\text{SSP}}(t)$ .

This method of SSP construction is nowadays known as the ‘isochrone method’ (Charlot & Bruzual 1991). Other approaches are also possible, as discussed by e.g. Rocca-Volmerange et al. (1996) and Lançon & Rocca-Volmerange (1996). A useful approximation derives from the observation that in a SSP the post-main sequence stars occupy a very limited interval of initial masses. Thus, all post-MS evolutionary phases can be described by a single stellar track, of initial mass similar to the SSP turn-off mass  $M_{\text{TO}}$ ; and all MS stars can be represented by a single ZAMS line of variable mass. With these approximations, equation (1) becomes

$$L_{\lambda}^{\text{SSP}}(t) = \int_0^{M_{\text{TO}}(t)} \phi_M L_{\lambda M}(0) dM + b(t) \int_{t_H}^{\infty} L_{\lambda M_{\text{TO}}}(\tau) d\tau, \quad (2)$$

where the second integral correspond to the integration over the post-MS part (i.e. with  $t > t_H$ ) of the evolutionary track of mass  $M_{\text{TO}}$ , and

$$b(t) = \phi_{M_{\text{TO}}} \left| \frac{dt_H}{dM_i} \right|_{M_i=M_{\text{TO}}}^{-1} \quad (3)$$

is the evolutionary flux, i.e., the number of stars which leave the MS by unit time (see Renzini & Buzzoni 1986). In the latter equation,  $t_H(M_i)$  is the main sequence lifetime as a function of the initial mass.

Equation 2, when written for the bolometric luminosity of a SSP, leads to the fuel consumption theorem as stated by Renzini & Buzzoni (1986): the second integral in the r.h.s. of equation (2) is replaced by the sum over a number  $n$  of evolutionary phases. Given the direct proportionality between the quantity  $L\Delta t$  for a single evolutionary phase  $j$ , and the nuclear fuel  $F_j$  consumed during it (the release of gravitational energy and neutrinos being neglected), equation (2) becomes

$$L_{\text{bol}}^{\text{SSP}}(t) = L_{\text{bol}}^{\text{MS}}(t) + A b(t) \sum_{j=1,n} F_j(M_{\text{TO}}), \quad (4)$$

where  $L_{\text{bol}}^{\text{MS}}(t)$  is a well-behaved function of time [see equation (2)], and  $A = 9.75 \times 10^{10} L_{\odot} \text{ yr } M_{\odot}^{-1}$  is a constant derived from the  $Q$ -value of H-burning reactions. The fuel consumption, in a first approximation, is then given by

$$F_j \simeq \Delta M_{\text{H}j} + 0.1 \Delta M_{\text{He}j}, \quad (5)$$

where  $\Delta M_{\text{H}j}$  and  $\Delta M_{\text{He}j}$  are the masses of H and He, respectively, nuclearly burned during the  $j$ -th evolutionary phase of the star of initial mass  $M_{\text{TO}}$ .

It can be noticed that the fuel consumption theorem involves a large number of approximations, with respect to the original equation (1). However, it provides us with a powerful tool for a qualitative understanding of the evolution of the integrated light of SSPs, since it relates  $L_{\text{bol}}^{\text{SSP}}(t)$

directly with the quantities  $F_j(M)$  derived from the stellar evolution theory. Nowadays the use of equation (1) to calculate integrated properties of SSPs is spread out due to the availability of several different sets of isochrones in the literature, but we can still rely on equation (4) in order to identify what causes the changes in the integrated magnitudes and colours. This is, basically, the approach adopted in this paper.

A concept useful to our analysis is that of the *total fuel consumption*, here defined as the fuel consumption summed over all the post-main sequence evolutionary phases:

$$F_T = \sum_{j=1,n} F_j. \quad (6)$$

The post-AGB phases can be left out from this definition because their fuel consumption is very small if compared to that from the preceding evolutionary stages. For the stars that finish their nuclear evolution as thermally pulsing AGB stars (i.e., for  $M_{\text{up}} > M \gtrsim 0.5 M_{\odot}$ ), the intershell mass at the end of the AGB,  $M_{\text{H}} - M_{\text{He}}$ , takes very small values if compared to  $M_c$  (typically, hundredths of solar masses at its maximum values during quiescent phases of H-burning, see e.g. Boothroyd & Sackmann 1988), and then from equation (5) we have

$$F_T \simeq 1.1M_c^{\text{AGB}} - M_c^{\text{MS}}, \quad (7)$$

where  $M_c^{\text{AGB}}$  and  $M_c^{\text{MS}}$  are the masses of the H-exhausted cores at the end of the AGB and MS evolution, respectively. We recall that  $M_c^{\text{MS}}$  is expected to be a well-behaving function of stellar masses, similarly to  $L_{\text{bol}}^{\text{MS}}$  which is a well-behaving function of age.

The latter equation allows us to draw already some conclusions about how the integrated near-infrared colours of SSPs vary with age. Combined with equation (4), equation (7) tells us that, for those SSPs that contain AGB stars (i.e. those with  $M_{\text{TO}} \lesssim M_{\text{up}}$ ), the evolution of the bolometric luminosity can be simply related to the final core mass attained by them.

We recall that the final core mass is also a quantity similar to the final stellar (or remnant) mass, since at the end of the AGB evolution only a very tiny envelope mass is left (of the order of thousandths of solar masses, see Schönberner 1981).

Therefore, we have an unique relation between the bolometric luminosity of the SSPs,  $L_{\text{bol}}^{\text{SSP}}(t)$ , and the final masses  $M_f \simeq M_c(t)$  of their AGB stars. If we have also a single initial-final mass relation  $M_f(M_i)$ , and a simple, monotonic relation between the initial mass and the SSP ages, then it follows that *the evolution of the bolometric luminosity of SSPs with  $M_{\text{TO}} \lesssim M_{\text{up}}$  will closely reflect the initial-final mass relation*. The same holds, to some extent, for the luminosities in the reddest photometric bands, since they sample the region of the spectrum which is dominated by the coolest and more luminous AGB stars, which are just those with the highest core masses. Therefore, the number of these stars, and their relative contribution to the near-infrared spectrum, are expected to vary also in correspondence with  $F_T$ . We can tentatively conclude that the evolution of the near-infrared luminosity (e.g. the *K* band), and of colours involving a visual and a near-infrared luminosity (e.g. the *V - K* colour), should have some correspondence with the

behaviour of the initial-final mass relation. We turn back to this point in Section 3.1.

## 2.2 Evolutionary tracks and AGB evolution

In this section we present the evolutionary tracks which we use in order to compute the integrated colours of SSPs. We include an overview of the properties which are relevant to the understanding of the colour evolution, in the framework provided by the fuel consumption theorem.

### 2.2.1 From the MS to the end of the early-AGB

We calculated two complete grids of stellar tracks of metallicities  $[Z = 0.001, Y = 0.23]$  and  $[Z = 0.008, Y = 0.25]$ , and with initial masses ranging from 0.15 to  $7 M_{\odot}$ . Initial stellar masses are spaced by  $0.1 M_{\odot}$  over the entire range of low-mass stars, and  $1.0 M_{\odot}$  in the range from 3 to  $7 M_{\odot}$ ; this spacing is reduced to  $0.05 M_{\odot}$  in the vicinity of  $M_{\text{Hef}}$ , and to  $0.5 M_{\odot}$  in the vicinity of  $M_{\text{up}}$ . This mass resolution is suitable to completely map the development of the tracks in the HR diagram, as well as to follow the growth of the core mass at the RGB-tip in the vicinity of  $M_{\text{Hef}}$ . It allows us to study the color evolution of SSPs even in some fine details.

The physical input of the models is as in the series of papers by Bressan et al. (1994a) and Fagotto et al. (1994a,b), with some updating in the equation of state, low-temperature opacities, and some of the nuclear reaction rates (Girardi et al. 1996). For the sake of brevity, we just recall here the main characteristics of the models. They are calculated with recent OPAL (Iglesias & Rogers 1996) and low-temperature opacities (Alexander & Ferguson 1994), and moderate convective overshoot from stellar cores (Bressan et al. 1994a and references therein). The equation of state includes both Coulomb interactions in the center (cf. Girardi et al. 1996), and the  $\text{H}_2$  molecule formation (cf. Mihalas et al. 1990 and references therein) in the coolest stars. The adoption of convective overshoot reflects on the lower values of the limiting initial masses for building degenerate cores after the exhaustion of central H and He: namely, we find  $M_{\text{Hef}} = 1.9 - 2.0 M_{\odot}$ , and  $M_{\text{up}} = 5 M_{\odot}$ , whereas classical models predict  $M_{\text{Hef}} \sim 2.2 M_{\odot}$  and  $M_{\text{up}} = 7 - 8 M_{\odot}$  (e.g. Sweigart et al. 1990; Iben & Renzini 1983). Another point is that we avoid any artificial discontinuity in the input parameters. For instance, the overshooting parameter (see Bressan et al. 1994a) is let to increase linearly from 0 up to its maximum value, 0.5, in the mass range  $1.0 < (M/M_{\odot}) < 1.5$ . In this way, the stellar lifetimes also behave as a smooth and monothonic function of stellar mass.

In the case of low-mass stars, evolutionary tracks are interrupted at the onset of the He-flash, and the corresponding HB track is continued from a ZAHB model with the same core mass and composition of the last RGB model.

Tables 1 and 2 present some of the characteristics of the  $Z = 0.001$  and  $Z = 0.008$  models which may be important to the considerations done in this paper. Data on the models with  $0.15 < (M/M_{\odot}) < 0.6$  are not presented since these are essentially non-evolving main sequence stars. Complete tables with the evolutionary tracks and derived isochrones will be published elsewhere, but are already available on request (e-mail: leo@mpa-garching.mpg.de).

**Table 1.** Lifetimes and core masses for the  $Z = 0.001$  stellar tracks.

$M_i$ ( $M_\odot$ )	$\tau_H$ (yr)	$M_c^{\text{RGB}}$ ( $M_\odot$ )	$\tau_{\text{He}}$ (yr)	$M_c^{\text{EAGB}}$ ( $M_\odot$ )
0.55	...	...	1.266e8	0.4951
0.60	40.87e9	0.4797	1.147e8	0.5030
0.65	...	...	1.136e8	0.5090
0.70	22.51e9	0.4772	1.197e8	0.5139
0.80	13.43e9	0.4762	1.181e8	0.5195
0.90	8.477e9	0.4740	1.199e8	0.5247
1.00	5.611e9	0.4721	1.072e8	0.5257
1.10	3.903e9	0.4711	1.079e8	0.5284
1.20	2.864e9	0.4698	1.158e8	0.5326
1.30	2.256e9	0.4691	1.062e8	0.5360
1.40	1.875e9	0.4676	1.126e8	0.5434
1.50	1.594e9	0.4660	1.127e8	0.5481
1.60	1.316e9	0.4359	1.247e8	0.5347
1.65	1.207e9	0.4105	1.558e8	0.5310
1.70	1.109e9	0.3431	2.341e8	0.5117
1.75	1.021e9	0.3336	2.314e8	0.5281
1.80	9.451e8	0.3289	2.222e8	0.5287
1.90	8.177e8	0.3262	1.943e8	0.5472
2.00	7.148e8	0.3300	1.714e8	0.5746
2.20	5.615e8	0.3471	1.240e8	0.6186
2.50	4.124e8	0.3835	0.767e8	0.6850
3.00	2.739e8	0.4567	0.427e8	0.8132
4.00	1.499e8	0.6254	0.183e8	0.8980
4.50	1.174e8	0.7172	0.130e8	0.9345
5.00	9.674e7	0.8206	0.976e7	0.9892
5.50	7.948e7	0.9297	0.639e7	1.5053
6.00	6.816e7	1.0419	0.584e7	1.7387
7.00	5.092e7	1.2930	0.341e7	2.0302
8.00	3.996e7	1.5741	0.249e7	2.4129

$M_i$  is the initial mass;  $\tau_H$  and  $\tau_{\text{He}}$  are the lifetimes for central H and He-burning, respectively ('e' denotes a power of 10);  $M_c^{\text{RGB}}$  and  $M_c^{\text{EAGB}}$  are the masses of the H-exhausted cores at the end of the RGB and E-AGB stages, respectively.

### 2.2.2 The TP-AGB evolution

We follow the TP-AGB evolution in an synthetic way (Iben & Truran 1978), starting from the last AGB model calculated along the evolutionary tracks. The total mass  $M$ , core mass  $M_c$ , effective temperature  $T_{\text{eff}}$ , and luminosity  $L$  of the models are let to evolve according to some analytical formulas which inter-relate these quantities and their time derivatives. The formulas are basically a subset of those collected by Groenewegen & de Jong (1993) and Marigo et al. (1996a). The end of the TP-AGB phase is determined either by the total ejection of the envelope by stellar winds, or by the core mass growing up to the limit for explosive carbon ignition,  $1.4 M_\odot$  (see however Section 2.2.4).

Without entering in the details about the integration procedure, we list here the complete set of ingredients of our TP-AGB models:

**Table 2.** The same as in Table 1, but for  $Z = 0.008$ .

$M_i$ ( $M_\odot$ )	$\tau_H$ (yr)	$M_c^{\text{RGB}}$ ( $M_\odot$ )	$\tau_{\text{He}}$ (yr)	$M_c^{\text{EAGB}}$ ( $M_\odot$ )
0.55	...	...	0.984e8	0.5103
0.60	57.43e9	0.4518	1.007e8	0.5120
0.70	32.85e9	0.4584	0.981e8	0.5187
0.80	18.94e9	0.4707	0.965e8	0.5220
0.90	11.88e9	0.4701	0.961e8	0.5245
1.00	7.691e9	0.4693	0.941e8	0.5254
1.10	5.064e9	0.4684	0.951e8	0.5280
1.20	3.666e9	0.4684	0.947e8	0.5288
1.30	2.945e9	0.4679	0.948e8	0.5311
1.40	2.450e9	0.4676	0.938e8	0.5323
1.50	2.077e9	0.4623	0.967e8	0.5312
1.60	1.706e9	0.4529	1.020e8	0.5262
1.70	1.426e9	0.4399	1.121e8	0.5234
1.80	1.217e9	0.4155	1.330e8	0.5109
1.85	1.127e9	0.4056	1.447e8	0.5094
1.90	1.043e9	0.3243	2.910e8	0.4962
2.00	9.097e8	0.3249	2.538e8	0.5001
2.20	7.038e8	0.3284	2.110e8	0.5094
2.50	5.088e8	0.3511	1.465e8	0.5407
3.00	3.270e8	0.4102	0.690e8	0.6204
3.50	2.289e8	0.4854	0.353e8	0.7574
4.00	1.699e8	0.5668	0.203e8	0.8716
4.50	1.317e8	0.6628	0.130e8	0.9177
5.00	1.051e8	0.7668	0.905e7	1.1379
5.20	9.656e7	0.8143	0.792e7	1.2125
5.50	8.596e7	0.8790	0.661e7	1.3275
6.00	7.189e7	1.0052	0.505e7	1.5772
7.00	5.264e7	1.2659	0.329e7	1.9626

**The core mass–luminosity relation (CMLR)** is from Groenewegen & de Jong (1993; and references therein):

$$L = \begin{cases} 2.38 \times 10^5 \mu Z_{\text{CNO}}^{0.04} (M_c^2 - 0.0305 M_c - 0.1802), & M_c < 0.7 M_\odot \\ 1.226 \times 10^5 \mu^2 (M_c - 0.46) M^{0.19}, & M_c > 0.95 M_\odot \end{cases} \quad (8)$$

where  $\mu = 4/(5X + 3 - Z)$  is the mean molecular weight, and  $Z_{\text{CNO}}$  is the mass fraction of CNO elements in the stellar envelope, in our case approximated by  $0.71 Z$ . In the  $0.95 \leq (M_c/M_\odot) \leq 0.7$  interval,  $L$  is interpolated linearly between the above relations.

For the first thermal pulses, when the star has a luminosity below that given by the CMLR, we use the same relation derived by Marigo et al. (1996a) from the Vassiliadis & Wood's (1993) models. From the last model of the evolutionary track, the luminosity and core mass of are extrapolated according to the relation

$$\frac{dL}{dM_c} = 60761 \exp(M/2) \quad (9)$$

until  $L$  equals the value given by the CMLR.

The breakdown of the CMLR, occurring in the AGB stars of higher masses (Blöcker & Schönberner 1991), will be thoroughly discussed in the next section. This effect does not occur in stars of mass lower than about  $3 M_\odot$ , for which the above relations are valid.

**The evolutionary rate**  $\dot{M}_c$  gives us the rate of core growth. According to Groenewegen & de Jong (1993; and references therein):

$$\dot{M}_c = 9.555 \times 10^{-12} \frac{L_H}{X} \quad (10)$$

where  $L_H$  is the luminosity of the H-burning shell during the quiescent phases of interpulse evolution, related to the total luminosity by

$$L = L_H + 2000(M/0.7)^{0.4} \exp[3.45(M_c - 0.96)]. \quad (11)$$

**The effective temperature**  $T_{\text{eff}}$  can also be given as a function of basic stellar parameters. Given the simplicity of our synthetic TP-AGB model, we need only the derivative of  $T_{\text{eff}}(L)$ , because an initial value of the effective temperature is given by the last evolutionary model we have in the complete stellar track. We choose a  $T_{\text{eff}}(L)$  relation with the same formal structure as that used by Renzini & Voli (1981), and differencing it with respect to  $L$  we obtain:

$$\frac{d \log T_{\text{eff}}}{d \log L} = \gamma(Z) + 0.017 \frac{d \log M}{d \log L}. \quad (12)$$

The coefficient 0.017 in this equation is the one which better fit our tracks for the early-AGB. Renzini & Voli instead use a coefficient of 0.08. The difference is probably due to the fact that the two estimates are derived from stellar models calculated with very different opacity tables and mixing length parameters. The  $\gamma(Z)$  function is obtained directly from the slope on the HR diagram of the complete evolutionary tracks at the stage of E-AGB, evolved at constant mass and for different metallicities. An equation like (12) guarantees both the continuity of the AGB tracks on the HR diagram, and a suitable dependence of the effective temperature on the total mass of the star. On the other hand, it can be an oversimplification of the real situation for TP-AGB stars of higher luminosities, where the envelope structure (and hence  $T_{\text{eff}}$ ) can be strongly modified by the products of third dredge-up and by the occurrence of hot bottom burning (e.g. Renzini & Voli 1981; Marigo et al. 1998). We hope, however, that equation (12) can be an useful first approximation for the kind of investigation we are interested in.

**The mass-loss rate**  $\dot{M}$  constitutes one of the most uncertain ingredients of the models of AGB stars. The classical Reimers' (1975) formula,

$$\dot{M} = 4 \times 10^{-13} \eta \frac{LR}{M}, \quad \eta \sim 1 \quad (13)$$

(with  $L$ ,  $R$  and  $M$  in solar units, here and throughout this section) is known not to provide the high mass-loss rates observed in real AGB stars, and required for the production of planetary nebulae at the end of the AGB (Iben & Renzini 1983). We consider here 3 other formulations for the mass-loss rates, all of them sharing the characteristic of developing a 'superwind' phase (with  $\dot{M} \gtrsim 10^{-5} M_{\odot}/\text{yr}$ ) at moderate luminosities. It follows a brief description of them.

(i) The Bowen & Willson (1991) prescription is based on the results of hydrodynamical models for the envelope of giant pulsating stars (Bowen 1988). It is characterized by an exponential increase of the mass-loss rate with the luminosity, or equivalently, with the pulsating period  $P$ . The Bowen

& Willson's results are not presented in the form of analytical formulas for the mass-loss rate as a function of relevant stellar parameters. However, the following formula is a fit to the results presented in their Fig. 2:

$$\log \dot{M} = \begin{cases} -4.925 \log M + 7.65 \log P - 26.08, & M \leq 1.2 M_{\odot} \\ -24.996 \log M + 7.08 \log P + & \\ \quad 7.198 \log M \log P - 24.489, & M \geq 1.2 M_{\odot} \end{cases} \quad (14)$$

This equation gives values for  $\dot{M}$  very close to those originally presented by Bowen & Willson (the maximum differences are of only  $\Delta \log \dot{M} = -0.14$ ). The pulsation period  $P$  (in days), can be obtained as a function of basic stellar parameters by means of Vassiliadis & Wood's (1993) period-mass-radius relation:

$$\log P = -2.07 + 1.94 \log R - 0.9 \log M. \quad (15)$$

(ii) The Blöcker's (1995) prescription was constructed with the aim of expressing the theoretical results of Bowen (1988) by means of a simple approximative formula:

$$\dot{M} = 4.83 \times 10^{-9} L^{2.7} M^{-2.1} \dot{M}_R, \quad (16)$$

where  $\dot{M}_R$  is the Reimers' mass-loss rate [equation (13)] with  $\eta = 1$ . In fact, comparing the results of equations (14) and (16) we notice that the latter gives values for  $\dot{M}$  that are typically much higher than those originally presented in Bowen's work.

(iii) Vassiliadis & Wood (1993) give a prescription for the mass-loss rates which is mostly based on observational data for long-period variables (Mira and OH/IR) stars. It relates  $\dot{M}$  with the pulsation period  $P$  (in days):

$$\log \dot{M} = -11.4 + 0.0123 P, \quad P \lesssim 500 \text{ days}. \quad (17)$$

For periods longer than  $\sim 500$  days, the mass-loss rate is given by the theory of radiation-driven winds, or

$$\dot{M} = 6.07 \times 10^{-3} \frac{L}{c v_{\text{exp}}}, \quad (18)$$

where  $c$  is the velocity of light, and  $v_{\text{exp}}$  is the wind expansion velocity,  $v_{\text{exp}} = -13.5 + 0.056 P$ , both in  $\text{km s}^{-1}$ . In our calculations the adopted mass-loss rate is the highest one between those given by (17) and (18).

The above relations are enough to describe the time evolution of the stellar parameters  $L$ ,  $T_{\text{eff}}$ ,  $M_c$  and  $M$  along the TP-AGB. It is worth recalling that this TP-AGB model is much simpler than, and probably not as accurate as, those presented in some recent papers in the literature (e.g. Groenewegen & de Jong 1993; Marigo et al. 1996a). However, our theoretical scheme is suitable to the main scope of this paper, which is to give an appropriate description of how the integrated colours of SSPs evolve with time. We notice, for example, that the results for the initial-final mass relation obtained by us adopting Vassiliadis & Wood's (1993) mass-loss rates, and in the case of  $Z = 0.008$ , are very similar to those derived by Marigo et al. (1996a). This despite the fact that the latter authors use a much more detailed TP-AGB model, which accounts for various effects such as the changes in the chemical composition at the stellar surface, and makes use of a complete envelope model in order

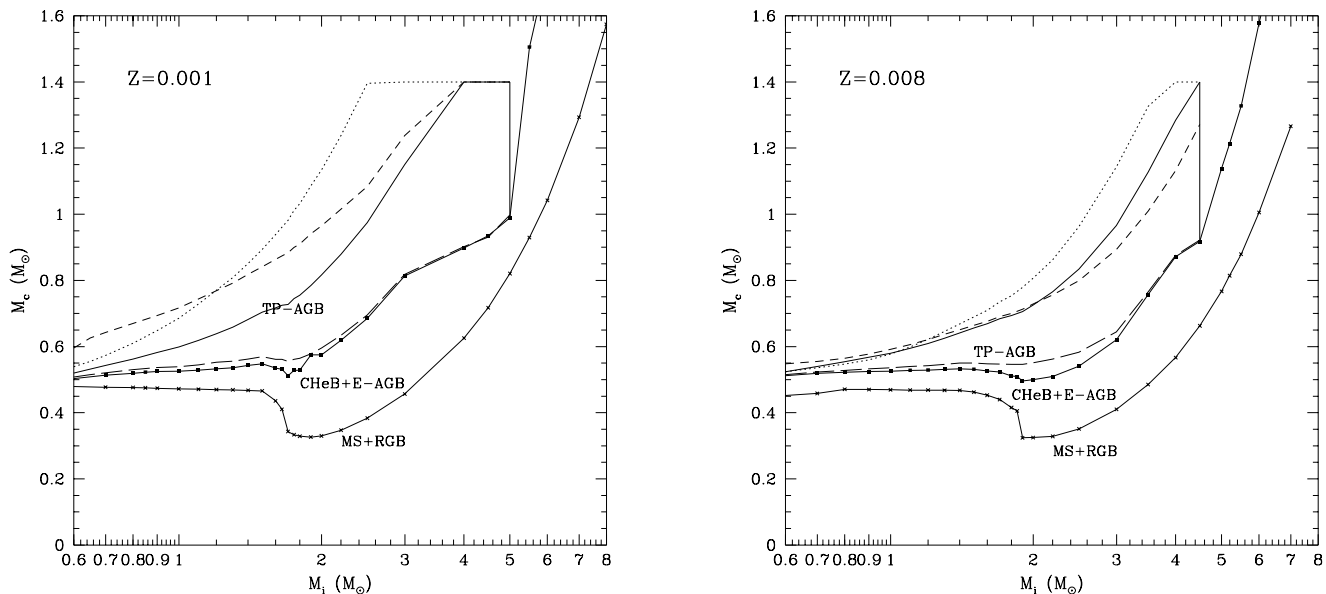


**Figure 1.** The He-core mass as a function of initial mass, at both the start of CHEB (RGB-tip for low-mass stars, or quiet He-ignition for intermediate-mass stars), and at the TP-AGB-end, for initial metallicities  $Z = 0.001$  (left panel) and  $Z = 0.008$  (right panel). The lines are as follows: the lower continuous line with crosses is the He-core mass at the beginning of the CHEB phase,  $M_c^{\text{RGB}}$ ; the continuous line with black dots immediately above is the core mass at the start of the thermally pulsing regime on the AGB,  $M_c^{\text{EAGB}}$ , or quiet C-ignition for high-mass stars; then follow the core mass at the end of AGB evolution (complete ejection of the envelope or supernova explosion) for 4 different prescriptions of mass-loss: Reimers (1975) with  $\eta = 1.0$  (continuous line), Bowen & Willson (1991; dotted line), Vassiliadis & Wood (1993; short-dashed line) and Blocker (1995; long-dashed line).

to obtain the effective temperatures. This agreement is encouraging, since the final core mass is a key-quantity for our colour evolution models [see equation (6)].

### 2.2.3 The core mass at several evolutionary stages

The final core mass built up at the end of the AGB,  $M_c^{\text{AGB}}$ , is highly dependent on the assumed mass-loss rates. Figure 1 shows the values of  $M_c^{\text{AGB}}$  for the 4 different formulations for the mass-loss presented in the above section.

In Fig. 1 it is clear that the Vassiliadis & Wood (1993) and Bowen & Willson’s (1991) mass-loss formulas, contrarily to the Reimer’s (1975) one, give origin to a strong metallicity dependence of the final core mass attained by intermediate-mass stars. In this way, stars of lower metallicity finally develop higher core masses, and can easily attain the critical core mass of  $1.4 M_\odot$ . This would result in supernova explosions of type I1/2 (Iben & Renzini 1983), with important implications for the theory of chemical evolution of galaxies (see Matteucci & Tornambè 1985). The Blocker’s (1995) formulation, instead, gives origin to very high values of mass-loss rates as soon as it is activated in the synthetic TP-AGB calculation. For this reason, in Fig. 1 the final core masses developed by models with this choice of mass-loss, are very close to the core masses at the start of thermal pulses. It stresses our conclusion that Blocker’s formulation for the mass-loss rates is indeed very different from the original ones obtained by Bowen (1988) and Bowen & Willson (1991).

We note on passing that models which use Vassiliadis &

Wood’s (1993) mass-loss rates were already shown to reproduce the maximum luminosity of AGB stars as a function of age in Magellanic Cloud clusters (cf. Marigo, Girardi & Chiosi 1996b), for ages  $8.8 \lesssim \log(t/\text{yr}) \lesssim 9.6$ . This provides also a useful constraint to mass-loss rates, since  $L$  and  $M_c$  are straightly linked by the CMLR. For this reason, and because it is based on observational data, we believe that Vassiliadis & Wood’s formulation for  $\dot{M}$  is probably the most realistic between those tested in this work. A conclusive test on the mass-loss rates is provided by a comparison of models with solar metallicity and the initial–final mass relation observed in the solar vicinity (Herwig 1996). In fact, tests made with  $Z = 0.02$  models revealed that TP-AGB stars with Reimers’ (1975) mass-loss rates end their evolution with too large core masses and luminosities, while those with Blocker’s (1995) mass-loss rates end with too small core masses.

An important aspect to be noticed in Fig. 1 and Table 1 is that

- the core mass at the beginning of the He-burning (corresponding to the RGB-tip for low-mass stars and to quiet He-ignition for intermediate- and high-mass stars),  $M_c^{\text{RGB}}$ , is a non-smooth function of initial mass. It presents the well-known plateau of  $M_c \simeq 0.45 M_\odot$  for  $M_i < M_{\text{Hef}}$ , a rapid jump from  $\sim 0.45$  to  $\sim 0.32 M_\odot$  in the vicinity of  $M_i \simeq M_{\text{Hef}}$ , and increases monotonically with the stellar mass for  $M_i > M_{\text{Hef}}$ ;
- on the contrary, irrespective of the adopted mass-loss formulation, *the final core mass attained by AGB stars,*

$M_c^{\text{AGB}}$ , is a smooth and monotonically increasing function of the initial stellar mass for the entire range of  $M_i < M_{\text{up}}$ .

It means that the He-burning evolution has the property of almost completely erasing the memory about the core mass at the earlier evolutionary stages. Most of this leveling-off effect takes place during the HB and E-AGB evolution, as can be noticed by looking at the lines in Fig. 1. The residual discontinuities in the function  $M_c(M_i)$  are smoothed out during the TP-AGB, as a natural result of

- (i) the existence of a core mass–luminosity relation during most of the TP-AGB evolution,
- (ii) of the fact that all mass-loss formulas are simply expressed as a regular function of fundamental stellar parameters as the effective temperature and luminosity, and
- (iii) of this mass-loss being a very steep function of the luminosity.

Considering the straight relation between the final core mass and the total fuel consumption of a star [cf. equation (7)], it implies that the total fuel consumption is also a smooth and monotonic function of the initial mass, even in the mass range in which the development of the RGB starts.

#### 2.2.4 The effect of AGB overluminosity

It is nowadays clear that the core mass-luminosity relation does not describe the luminosity evolution of all AGB stars. Tuchman, Glasner & Barkat (1983) clarified that the validity of the CMLR depends on the existence of a radiative region between the H-burning shell and the convective envelope. For the AGB stars of higher masses, significant burning through the CNO cycle can occur at the bottom of the convective envelope, thus breaking down the validity of the CMLR for these stars, and allowing their luminosities to grow apparently unconstrained (Blöcker & Schönberner 1991; Boothroyd & Sackmann 1992). We will refer to this behaviour as the ‘AGB overluminosity’. Its effect on AGB evolution can be qualitatively understood as follows:

- (i) At the beginning of the TP-AGB, the star starts nuclear burning at the bottom of the envelope, and grows rapidly in luminosity ignoring the limitation imposed by the CMLR;
- (ii) the high luminosities soon trigger high mass-loss rates;
- (iii) once a significant amount of stellar mass has been lost, the conditions for envelope burning being active no longer exist, and the star goes down in luminosity up to attaining the CMLR;
- (iv) the star evolves along the CMLR, just as if it were an AGB star of lower initial mass. Conditions for reactivating the envelope burning are probably not met again up to the end of its life.

This kind of behaviour can be found e.g. in the  $5 M_{\odot}$  models computed by Vassiliadis & Wood (1993), in those of Boothroyd & Sackmann (1992), Blöcker (1995), and more recently in Marigo et al. (1998). The net result, according to the simplified picture above presented, is that AGB stars with high initial mass pass through a temporary phase of high luminosity, but soon after settle on an evolutionary behaviour which is in many aspects similar to those of AGB

stars born with lower initial masses. Thus, the final core mass attained by these stars is *lower* than that which would be attained if the CMLR were always valid for them. The same holds for the total fuel consumption, according to equation (7). Notice that a probable consequence of the overluminosity effect is that of preventing the core mass of AGB stars of growing up to the limit of  $1.4 M_{\odot}$ , thus accounting for the non-observation of supernovae of type I 1/2, even at very low metallicities.

The consideration of the overluminosity effect in synthetic calculations of the TP-AGB evolution is not an easy task. Complete evolutionary calculations indicate that the efficiency of envelope burning, as well as the amount of overluminosity, depends critically on a series of parameters as the envelope mass, core mass, metallicity and mixing length parameter (Sackmann & Boothroyd 1991; Boothroyd & Sackmann 1992; Boothroyd, Sackmann & Ahern 1993). At present, the only attempt to provide analytical formulas feasible to describe the luminosity increase of envelope burning stars, as a function of these parameters, is that from Wagenhuber & Groenewegen (1997).

In order to test the effect that the overluminosity effect can have on integrated colours of SSPs, we would like to present here calculations made under very simplified assumptions. We think that these experiments are worth because, up to this moment, the overluminosity effect was not considered in this kind of models. The simplest assumptions we can work with are that the overluminosity takes place in one of the following cases:

- (i) when the core mass is higher than  $0.85 M_{\odot}$ ;
- (ii) when the envelope mass is higher than  $1.6 M_{\odot}$ .

Case (i) corresponds to the statement originally made by Blöcker & Schönberner (1991) and Boothroyd & Sackmann (1992). It dates from the very first papers which dealt with envelope burning stars. It is now clear that this rule does not hold always: for instance, the Vassiliadis & Wood’s (1993) models with an initial mass of  $5 M_{\odot}$  have  $M_c \gtrsim 0.95 M_{\odot}$  and still follow a CMLR at the end of their evolution. These authors conclude that below certain values of envelope mass the hot bottom burning does not occur. This result is represented by the case (ii) above.

Let us consider that the envelope mass is the main determinant factor of the overluminosity, and assume a value of 50 percent of overluminosity for envelope masses in excess of  $0.4 M_{\odot}$ , so we have:

$$\frac{L}{L_{\text{CMLR}}} = 1 + 0.5 \frac{(M_A/M_{\odot} - 1.6)}{0.4},$$

for  $M_A = \max(M_{\text{env}}, 1.6 M_{\odot})$ . (19)

As an alternative formulation, we consider core masses in excess of  $0.85 M_{\odot}$  as a concurrent factor for the overluminosity:

$$\frac{L}{L_{\text{CMLR}}} = 1 + 0.25 \frac{(M_B/M_{\odot} - 0.85)}{0.1} \frac{(M_A/M_{\odot} - 1.6)}{0.4},$$

for  $M_B = \max(M_c, 0.85 M_{\odot})$ . (20)

Introducing these prescriptions in our equations for the stellar luminosities, we generate synthetic AGB models which attain the core masses illustrated in Fig. 2. We plot only the results obtained for the Vassiliadis & Wood (1993) mass-loss formulation. It can be noticed that these

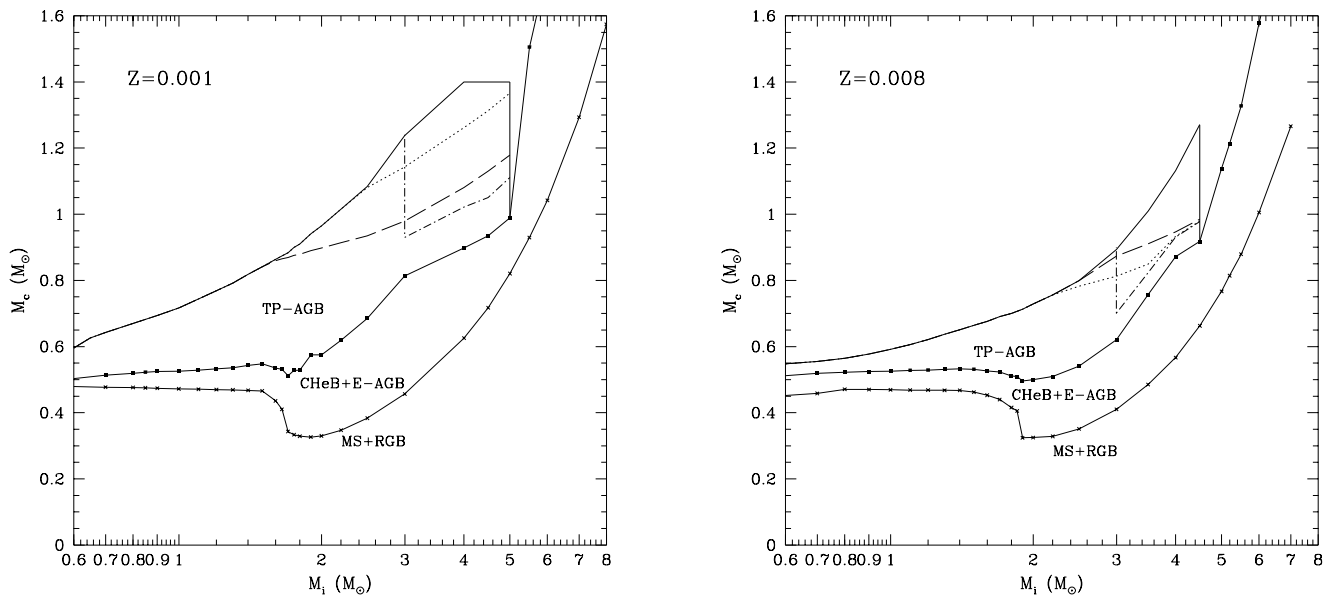


**Figure 2.** The same as Fig. 1, but limited to the case of Vassiliadis & Wood’s (1993) mass-loss rates, and considering the overluminescence effect on the most massive AGB stars according to 2 different prescriptions: as if the envelope mass were the only parameter determining the overluminescence [equation (19); dotted line], and as if the core mass also plays a role in the overluminescence effect [equation (20); long-dashed line]. For comparison, the curve obtained with the assumption of the validity of the CMLR (Fig. 1) is presented as a continuous line. The dotted-dashed line, instead, illustrates the predictions by Renzini (1992), according to whom the overluminescence effect reduces drastically the AGB lifetime for stars above a certain initial mass value. At sufficiently low masses, all the different models present the same final core masses.

prescriptions for the overluminescence cause a flattening of the initial–final mass relation for the most massive intermediate-mass stars (with  $M_{\text{up}} \gtrsim M_i \gtrsim 2.5 M_{\odot}$  for  $Z = 0.008$ ). We recall that some authors have suggested that the initial–final mass relation observed in the solar vicinity presents some evidences of such a flattening (see Herwig 1996; Jeffries 1997). For the stars in the vicinity of  $M_{\text{up}}$ , the AGB lifetime is shortened by a factor of up to 5. For the stars of lower masses, the overluminescence effect causes a progressive reduction of the AGB lifetime. For  $M_i \lesssim 2.5 M_{\odot}$ , the CMLR results to be valid through the entire AGB evolution.

The amount of overluminescence predicted by equations (19) and (20) are quite high if confronted to those found by several authors. However, we preferred to explore the most extreme possible conditions, since the results that would be obtained with more conservative assumptions, of course, would approach the results obtained in the case of no overluminescence. The reader should keep in mind the possibility of intermediate behaviours for the curves depicted in Fig. 2, which would also reflect on the results presented below.

### 2.2.5 Theoretical isochrones

Isochrones are constructed from the stellar tracks by means of a simple interpolating algorithm. The smooth and regular behaviour of the isochrones in the HR diagram is guaranteed by interpolating between points of equivalent evolutionary status over the stellar tracks, and by using  $\log M_i$  and  $\log t$  as the variables of interpolation. The procedure is similar to that used by Bertelli et al. (1994). The transformation from

the theoretical to the observed stellar quantities is also performed as in Bertelli et al. (1994), to whom we refer for all details. Suffice it to say that they rely on the Kurucz’s (1992) library of stellar spectra, complemented at low effective temperatures with observed spectral energy distributions from several authors. Giant stars are attributed  $V - K$  colours according to Bessell & Brett (1988) and Terndrup et al. (1991), and the  $T_{\text{eff}}$  scale from Lançon & Rocca-Volmerange (1992).

## 3 EVOLUTION OF INTEGRATED COLOURS

We now start discussing how the integrated colours evolve, in the different cases previously described. We recall that our models contain all the evolutionary phases relevant for the determination of the optical and near-infrared colours of SSPs.

Figure 3 shows, for two metallicity values ( $Z = 0.001$  and  $Z = 0.008$ ), the evolution of the  $B - V$  and  $V - K$  colours derived from a sequence of isochrones calculated with a very fine age spacing, for the entire age interval in which AGB stars are present. The several formulations for the mass-loss rates discussed in Section 2.2.2 are considered in this plot. These models correspond to those presented in Fig. 1. Figure 4, instead, shows the colour evolution for models which assume the Vassiliadis & Wood’s (1993) mass loss rates, and that consider the effect of overluminescence of the most massive AGB stars according to the prescriptions discussed in Section 2.2.4. It corresponds to the models shown

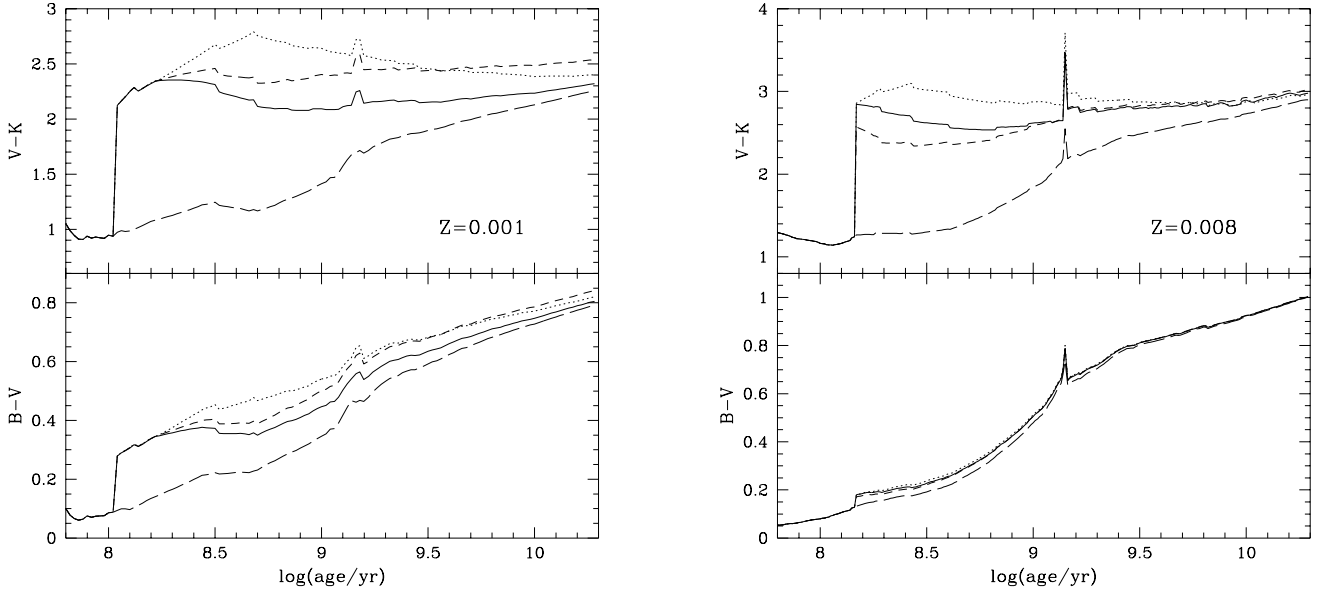


**Figure 3.** The time evolution of the  $B - V$  and  $V - K$  colours, for SSPs with metallicities  $Z = 0.001$  and  $Z = 0.008$ , and according to 4 different choices for mass-loss rates along the TP-AGB: Reimers (1975) with  $\eta = 1.0$  (continuous line), Bowen & Willson (1991; dotted line), Vassiliadis & Wood (1993; short-dashed line) and Blöcker (1995; long-dashed-line). The age interval shown covers entirely (and is slightly larger) that in which AGB stars are present in the SSPs. The features in the colour evolution at ages slightly larger than  $10^8$  and  $10^9$  yr, are associated with the onset of AGB and RGB stars, respectively (see text for details).

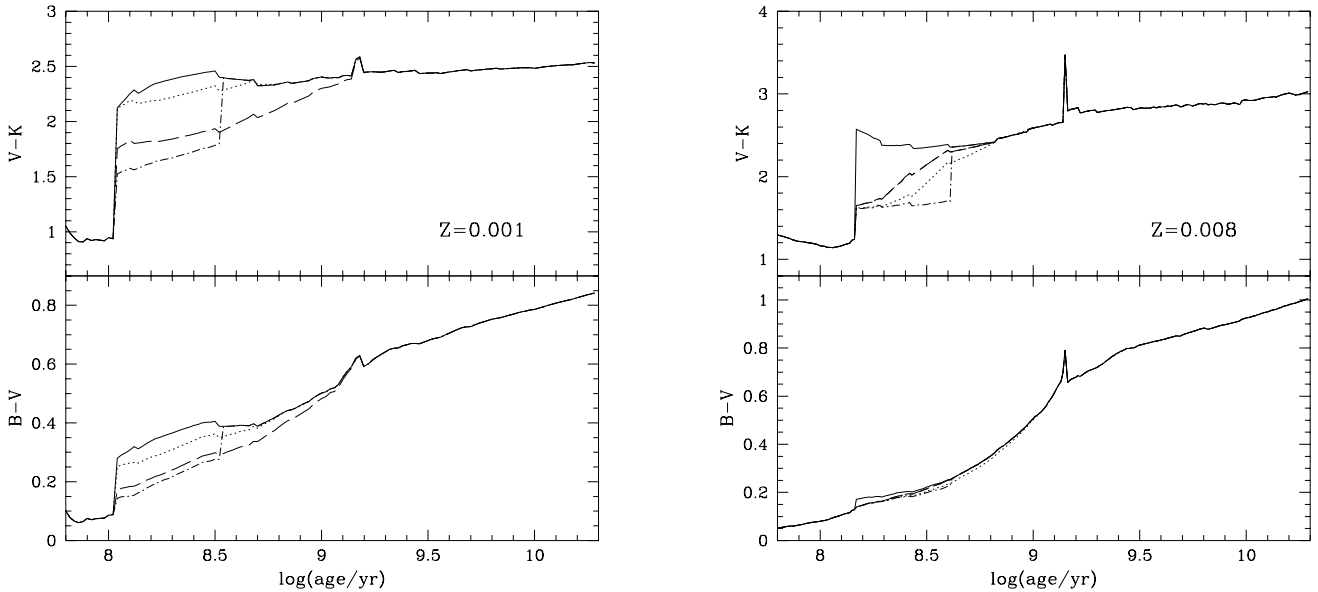


**Figure 4.** The same as Fig. 3, but limited to the case of Vassiliadis & Wood's mass-loss rates, and considering the overluminosity effect on the most massive AGB stars according to 2 different prescriptions: as if the envelope mass were the only parameter determining the overluminosity [equation (19); dotted line], and as if the core mass also plays a role in the overluminosity effect [equation (20); long-dashed line]. The continuous line shows the result for the case in which the overluminosity effect were ignored. The dotted-dashed line, instead, illustrates the predictions by Renzini (1992), according to whom the colour jump associated with the AGB phase transition would be split into two separate colour jumps. At sufficiently young and old ages, all the different models follow a common colour evolution.

in Fig. 2. Most of the considerations below refer to the results presented in these key figures.

All the SSP models are calculated assuming the simple Salpeter initial-mass function,  $\phi_{M_i} \propto M_i^{-2.35}$ . As demonstrated in e.g. Girardi & Bica (1993), integrated colours of SSPs, for ages  $t \gtrsim 10^8$  yr, depend only weakly on the assumed IMF slope.

### 3.1 The AGB phase transition

#### 3.1.1 The simplest case: results for canonical AGB evolution

The ‘AGB phase transition’ refers to the almost sudden change in the evolutionary behaviour of stars, that follows the development of a electron degenerate CO core prior to the carbon ignition (Renzini & Buzzoni 1986). It represents a real bifurcation in the evolutionary tracks in stars of mass  $M_i \simeq M_{\text{up}}$ : if  $M_i > M_{\text{up}}$ , the star follows a fast evolutionary history, in which C and O burning proceeds without a significant increase in  $M_c$ ; if on the contrary  $M_i < M_{\text{up}}$ , a relatively long evolutionary phase (the AGB) follows with the possibility of a substantial increase in  $M_c$  before its end. It results in an increase in the nuclear fuel at a quite precise value of initial mass. As this increase occurs only in the form of red stars, it causes the SSP colours – specially the reddest ones – to jump to the red at the age of  $t(M_{\text{up}})$ .

This is the classical view of the AGB phase transition, as idealized by Renzini & Buzzoni (1986) and found in a series of SSP models (e.g. Charlot & Bruzual 1991; Bressan et al. 1994b). Figure 3 illustrates clearly the pronounced jump in the  $V - K$  colour that occurs at an age of  $t(M_{\text{up}}) = 10^8$  yr, and how its magnitude depends on the prescription we adopt for the TP-AGB models. In near-solar metallicity SSPs, the  $B - V$  colour (as well as other ‘visual’ colours) is little affected by the onset of the AGB. This because MS and CHeB phases dominate completely the colour evolution at these pass-bands. The same does not occur for low-metallicity SSP models: as the AGB phase develops at relatively high effective temperatures in this case, also the  $B - V$  colour is strongly affected by the development of the AGB, as well as by all the uncertainties in the AGB evolution.

#### 3.1.2 The overluminescence affecting the AGB phase transition

Recently, Renzini (1992) suggested that the appearance of the colour jump associated with the AGB phase transition could be significantly delayed, thanks to the overluminescence effect that occurs in the most massive AGB stars. His argument is essentially that the overluminescence causes a strong reduction (up to a factor of 10) in the lifetime of the AGB stars that experience this effect. Thus, the amplitude of the colour jump at  $t(M_{\text{up}})$  would be reduced by a similar numerical factor, and a major jump in the colours would instead occur at a later age, corresponding to the advent of the first AGB stars that do not pass through the overluminescent phase. The limit mass for this ‘normal’ AGB evolution to occur was estimated to be  $3 M_{\odot}$ , and then the major colour jump due to the AGB development would occur at ages close to those of the RGB phase transition (remember

that according to classical models,  $M_{\text{Hef}} \simeq 2.2 M_{\odot}$ ). The situation is also illustrated in Fig. 4.

However, Renzini’s (1992) analysis does not consider an effect that became clear in subsequent papers about AGB evolution: that overluminescent stars sooner or later loose enough mass so that they go down in luminosity and follow a normal CMLR later on (see Section 2.2.4). This behaviour suggests that there is no clearcut transition from one evolutionary regime to the other (i.e., from overluminescent to normal) as we vary the initial stellar masses. On the contrary, the expected behaviour is that the overluminescence affects the AGB evolution (and hence integrated colours) less and less as we move from higher to lower initial masses (and hence from younger to older ages). We can appreciate this smooth transition in Fig. 2, where the overluminescence effect causes a flattening in the initial–final mass relation, instead of causing discontinuities in it. The same flattening effect occurs in the integrated colours, as shown in Fig. 4.

Therefore, although knowing the limitations of the present models (Section 2.2.4), we propose the interpretation that the overluminescence with respect to the CMLR causes a *temporal widening* of the colour jump associated to the AGB phase transition, and not its splitting into two separate events. More specifically, we suggest that after a colour jump of small amplitude at  $10^8$  yr, there would follow a gradual reddening of the integrated colours up to ages  $\sim 3 \times 10^8$  yr. After that age the overluminescence effect would not be found in the AGB stars present in the SSPs, and the colour evolution would follow strictly the curves depicted in Fig. 3. The age of  $3 \times 10^8$  yr corresponds to a turn-off mass of  $3 M_{\odot}$ . This is a sort of lower limit to the values found in the literature (e.g. Renzini & Voli 1981; Vassiliadis & Wood 1993; Wagenhuber 1996; Marigo et al. 1996a, 1998) as the limit mass for the presence of envelope burning in TP-AGB stars.

Comparing the different curves for  $(V - K)(t)$ , depicted in Figs. 3 and 4, with the corresponding curves for  $M_c^{\text{AGB}}(t)$  in Figs. 1 and 2, the reader can notice that the behaviour predicted by means of the fuel consumption theorem in Section 2.1, is in fact verified: the change in the  $V - K$  colours due to the presence of the AGB is proportional to the amount of increase in the core mass during this evolutionary phase. For instance, for  $Z = 0.008$  an increase of the core-mass of  $\Delta M_c = 0.5 M_{\odot}$  during the AGB causes an increase of  $\Delta(V - K) = 1.6$  mag in the  $V - K$  colours of the SSPs of corresponding age. The numerical ratio  $\Delta(V - K)/\Delta M_c$  is roughly constant for a given set of metallicities, and equal to 3.2 for  $Z = 0.008$ , and 3.0 for  $Z = 0.001$ . This suggests that the colour evolution of low-metallicity stellar populations, if observed, could provide us with useful constraints to the initial-final mass relationship at other metallicities. Although it may seem rather speculative, the star clusters of the SMC would be the obvious target for a study of this kind.

### 3.2 The RGB phase transition

Contrarily to the case of the AGB phase transition, the effect of the development of the RGB on the integrated colours has been debated over the years. Renzini & Buzzoni (1986) argued that a colour jump to the red should occur, based on the following characteristic features of the stellar models: (1) the fuel consumption in stars with  $M_i \leq M_{\text{Hef}}$  should

supposedly increase, due to the development of an extended RGB phase in which the core mass significantly increases; (2) the advent of degenerate He cores imply changes on the distribution of the red stars in the HR diagram, namely the development of the RGB and the increase of the HB (or CHeB) luminosity by about 0.4 magnitudes. All these features seem to imply a jump of the integrated SSP colours to the red at  $t(M_{\text{HeF}})$ .

The first complete models of stellar populations to investigate the behaviour of the colours in the relevant age interval (Chiosi et al. 1988; Charlot & Bruzual 1991), brought doubts about the occurrence of such a colour jump, or at least severely limited its possible amplitude. Chiosi et al. (1988) and Bressan et al. (1994b) argued that the RGB development is accompanied by a correspondent reduction in the contribution of the AGB to the integrated light, so that no significant effect in the colours could result from the increase in the fuel consumption on the RGB.

### 3.2.1 Results from complete SSP models

Let us now look at the problem with the aid of our models. In Fig. 3 the evolution of SSP colors is shown for a sequence of isochrones calculated with a very small age spacing. In the vicinity of the age at which the RGB develops,  $t(M_{\text{HeF}}) \simeq 10^9$  yr, the following characteristics are noticed:

- (i) the colors immediately before and after the onset of the RGB follow an apparently continuous and regular evolution;
- (ii) there is a small, bump-like excursion to red colors at an age slightly larger than  $t(M_{\text{HeF}})$ .

The first characteristic, (i), was already described in the works by Chiosi et al. (1988) and Bressan et al. (1994b): it reflects the continuity of the total fuel consumption for stellar populations which contain AGB stars [see Section 2.1, specially equation (6)]. To be more clear, we recall that what happens at the onset of the RGB is not a net increase in the total fuel consumption, but a simple rearrangement of the fuel burned by several evolutionary phases: a certain amount of fuel that for  $M_i > M_{\text{HeF}}$  was burned on the CHeB and AGB phases, for  $M_i < M_{\text{HeF}}$  is burned during the RGB phase. Most of the rearrangement occurs by the transference of fuel from CHeB and E-AGB stars to the RGB; the TP-AGB phase afterwards just levels off the remaining discontinuities in the function  $F_{\text{T}}(M_i)$  (see Section 2.2.3). And since RGB and E-AGB stars have virtually the same spectral energy distribution, the integrated colors do not suffer noticeable changes due to the RGB phase transition. A result that may be surprising, is that this behaviour is valid even for the near-IR colors.

The second characteristic – the bump-like excursion to the red, (ii) –, as far as we know, was not pointed out previously. It can be found only in SSP sequences built with a very small age spacing. The first impression one may have is that it could be a numerical error rather than a real feature of the colour evolution; we however verified that this is not the case. Apparently, its occurrence is not predicted from the straight application of the fuel consumption theorem.

In order to clarify the origin of this feature, we present in Fig. 5 the theoretical luminosity functions for isochrones located in the relevant age interval. The great increase in

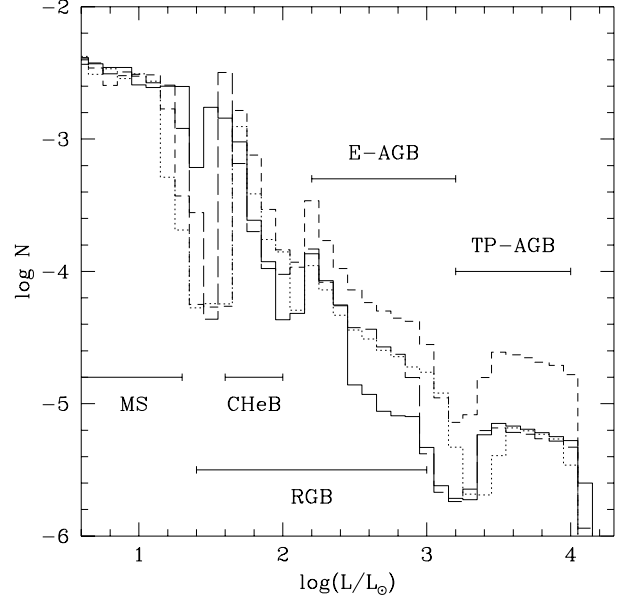


**Figure 5.** The luminosity functions for 4 isochrones with  $Z = 0.008$ . They have increasing ages of  $\log(t/\text{yr}) = 9.05, 9.10, 9.15,$  and  $9.2$  (respectively, the continuous, long-dashed, short-dashed and dotted lines). This age interval goes from the development of the RGB up to the end of the red phase depicted in Fig. 3. Notice the short RGB present in the  $\log(t/\text{yr}) = 9.05$  isochrone, and the increased number of AGB stars in the  $\log(t/\text{yr}) = 9.15$  one.

the number of AGB stars at the peak of the red phase is remarkable. This temporary excess number of AGB stars is the main responsible for the red phase, and can be understood according to the following.

The rate of birth of AGB stars in a SSP can be defined similarly to the evolutionary rate  $b(t)$  of equation (3):

$$\begin{aligned}
 b^{\text{AGB}}(t) &= \phi_{M_{\text{eHe}}} \left. \frac{dt_{\text{eHe}}}{dM_i} \right|_{M_i=M_{\text{eHe}}}^{-1} \\
 &\simeq \phi_{M_{\text{TO}}} \left. \frac{dt_{\text{eHe}}}{dM_i} \right|_{M_i=M_{\text{TO}}}^{-1}.
 \end{aligned} \quad (21)$$

where the subscript ‘eHe’ refers to the quantities evaluated at the end of the CHeB phase. Figure 6 shows a plot of the functions  $t_{\text{H}}(M_i)$  and  $t_{\text{eHe}}(M_i)$  for our  $Z = 0.008$  evolutionary tracks, over a limited range of ages and initial masses. We can notice that, while  $t_{\text{H}}$  is a quite regular function,  $t_{\text{eHe}}$  flattens at an age of about  $\log(t/\text{yr}) = 9.15$ . It causes the increase in  $b^{\text{AGB}}(t)$  at that age, and hence the red phase in the SSP colours. This particular behaviour of  $t_{\text{eHe}}$  occurs because the He-burning lifetime,  $t_{\text{He}}$ , is shortened from  $\sim 2 \times 10^8$  to  $10^8$  yr after the RGB develops (see Table 1).

The age of the red feature does not coincide exactly with the age in which the RGB first appears. In the  $Z = 0.008$  models, it occurs at  $9.14 \lesssim \log(t/\text{yr}) \lesssim 9.16$ , while the RGB develops completely over the age interval  $9.03 \lesssim \log(t/\text{yr}) \lesssim 9.08$ . This delay corresponds to the time lag between the ages in which the stars with  $M_i = M_{\text{HeF}}$  are either RGB (RGB development) or AGB stars (red phase), which can

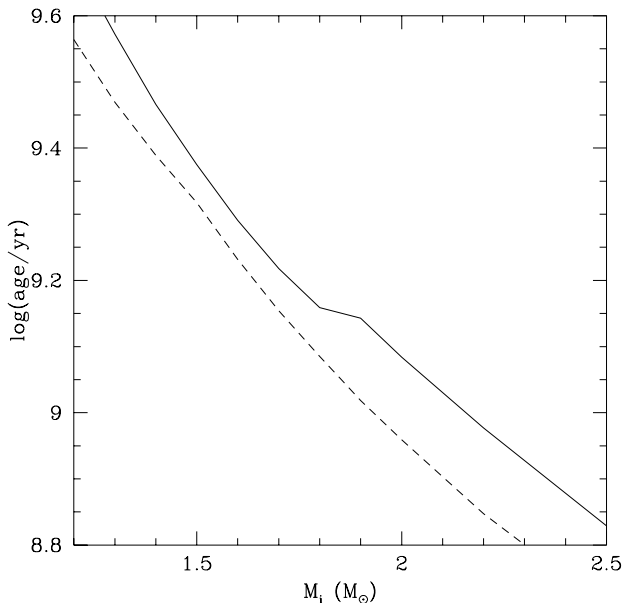


**Figure 6.** The lifetimes of the  $Z = 0.008$  stellar tracks up to the end of the main sequence,  $t_H$  (dashed line), and up to the end of the CHeB,  $t_{eHe}$  (continuous line). Notice in particular the flattening of the  $t_{eHe}(M_i)$  relation for ages  $\log(t/\text{yr}) \simeq 9.1$ .

be estimated as being similar to the He-burning lifetime, or  $\sim 1.5 \times 10^8$  yr.

We can conclude that a feature in the colour evolution takes place because the CHeB lifetime  $t_{He}(M_i)$  is strongly reduced in the vicinity of  $M_i = M_{HeF}$ . This is equivalent to the condition that a steep gradient in the function  $M_c^{RGB}(M_i)$  occurs at the onset of degenerate He-cores (Fig. 1). Naturally, a steeper gradient would favour red phases of higher amplitude, but also correspondingly shorter-lived.

We notice, moreover, that it is necessarily a transient effect, which may not be confused with the jump to redder colours predicted by Renzini & Buzzoni (1986) as a consequence of the RGB development. In the framework provided by the fuel consumption theorem, the temporary red phase we found may be understood as a second-order effect of the redistribution of the total fuel consumption  $F_T$  between the red giant stars present in the SSPs. But no long-lasting increase in this quantity takes place, therefore no effective colour-jump occurs.

### 3.2.2 Further remarks on the RGB phase transition

The red phase we found is probably the most important consequence of the so-called RGB phase transition in the colours of SSPs. But its transient nature imposes difficulties for its possible detection in real stellar populations. In the following we consider two different cases of astrophysical interest, for which the development of the RGB was previously claimed to possibly produce important observational counterparts. These are (1) the gaps in the color distribution of Magellanic Cloud star clusters, and (2) features in the colour/luminosity distribution of galaxies at large redshifts.

We think that this red phase can not cause gaps in the distribution of integrated colors of star clusters, as it would be the case if it were a real transition. More probably, it is a source of color dispersion, mixing some clusters with age  $\sim 10^9$  yr with their redder (older) neighbours in two-color planes. The number of clusters that could be affected by this effect, however, is limited by the relatively short duration of the red excursion. As an illustrative case, let us consider the *UBV* color distribution of LMC star clusters. In Fig. 3 we can notice that for the  $B - V$  colour and at  $Z = 0.008$ , the red phase manifests as a small bump in the colour evolution at ages of 1 Gyr, which amplitude does not exceed 0.05 mag. The work by Girardi et al. (1995) indicates that, for a sample of coeval clusters of similar ages, the intrinsic color spread due to stochastic effects is of  $\sim 0.02$  mag in  $B - V$ ; that due to a metallicity dispersion of 0.4 dex is of  $\sim 0.08$  mag, and  $\sim 0.1$  mag can be expected from the variations of the foreground reddening (these values are typical for the rich LMC clusters). Thus, the distribution of intrinsic properties of the LMC star clusters causes a color dispersion which is already higher than that could be caused by the red phase. The colour dispersion would then completely mask this small feature in the colour evolution. For this reason, we think that gaps in the distribution of  $B - V$  colors, as e.g. the one noticed by Bica et al. (1991), probably can not be formed as a consequence of the red phase. The same holds for the near-infrared colours, since for them the colour dispersion due to stochastic effects gets very high (e.g. Santos Jr. & Frogel 1997).

In a galactic population, two of the possible factors of color dispersion above considered disappear: (1) the stellar statistics is much higher, and (2) the reddening, either internal or foreground, is expected to have a smooth distribution, affecting equally all the components of the population. Even in this case, the red phase would reflect in the evolution of the galactic colours only if

- (i) the components of the galactic population were coeval, to within  $\sim 10^8$  yr; (Probably not even the oldest elliptical galaxies are expected to have formed on so short timescales.)
- (ii) the red phase were to appear at equal ages in SSPs of different metallicities, within the typical metallicity interval that composes a galaxy.

As none of these conditions is likely to occur, we conclude that the red phase does not provide a useful ‘evolutionary clock’, in the sense idealised by Renzini & Buzzoni (1986).

## 4 THE NEAR-INFRARED EVOLUTION OBSERVED IN LMC CLUSTERS

The rich star clusters of the Magellanic Clouds provide the most significant data for testing SSP models. They span a wide range of ages, being at the same time rich enough so that stars in some of the fast evolutionary stages are sampled. Moreover, for a reasonable number of these clusters, metallicities and ages have been determined with a good precision, by means of both spectroscopy of the red giant stars and CCD photometry down to the main sequence. For the large number of clusters for which only integrated photometry is available, ages can be estimated by means of the observed relationships between integrated photometric pa-

parameters and age, calibrated with the data for the best studied clusters. The most popular among these methods are the SWB classification scheme of Searle, Wilkinson & Bagnuolo (1980), based on *uvgr* photometry, and the *S* parameter of Elson & Fall (1985), based on *UBV* photometry.

Persson et al. (1983) observed 84 rich star clusters of both Magellanic Clouds in integrated *JHK* photometry. The combination of this data with the *UBV* photometry of other authors (see van den Bergh 1981; Bica et al. 1996) provides the basic dataset for the study of the evolution of the  $V - K$  colour. Persson et al. were the first to call attention to the apparent jump of the  $V - K$  colour from values  $\sim 1.5$  to  $\sim 3$ , occurring for star clusters of SWB type IV. This remains, basically, the main aspect of the data to be described by SSP models.

Other characteristic of the observational data was the large dispersion in the IR colours for clusters of the same SWB type (and hence similar age). Although part of this dispersion can be attributed to observational errors, it is clear that most of it derives from the natural dispersion in the number of evolved stars present in the clusters. In the theoretical models, this effect can be easily simulated by means of stochastic fluctuations in the initial mass function of model clusters (cf. Barbaro & Bertelli 1977; Chiosi et al. 1988; Girardi et al. 1995; Santos Jr. & Frogel 1997). These effects on the dispersion of near-IR colours of Magellanic Clouds clusters have been recently studied by Santos Jr. & Frogel (1997). In this paper, instead, we focus on the study of the mean evolution of the colours as a function of age.

#### 4.1 The data about cluster ages

In order to study the evolution of the near-infrared colours of MC clusters, we must first properly rank the clusters observed by Persson et al. (1983) into an age sequence. The latter authors based their own age ranking on a subdivision of the SWB classification (Searle et al. 1980). More precisely, they drew over the  $Q_{ugr} \times Q_{vgr}$  diagram of Searle et al. (1980; see Fig. 1 in Persson et al. 1983) a mean ridge line through the distribution of star clusters, scaling it by means of an age parameter  $t_{\text{PACFM}}$  from 0 to 300. Then, a value of  $t_{\text{PACFM}}$  was attributed to each cluster by projecting it over the mean line. The assumption that  $t_{\text{PACFM}}$  represents really an age sequence, derives from the demonstration by Searle et al. (1980), that their mean SWB groups (also defined in the  $Q_{ugr} \times Q_{vgr}$  diagram) represent a sequence of increasing age and decreasing metallicity.

Another approach is that followed by Elson & Fall (1985). They have drawn a similar ridge line along the distribution of star clusters in the integrated  $(U - B)$  vs.  $(B - V)$  plane, attributing to each cluster an age parameter  $S$ . The relationship between  $S$  and the logarithm of the age was found to be linear, and was calibrated by using a large amount of photometric data (see also Elson & Fall 1988). Girardi et al. (1995) have revised the method, basically confirming its validity. Two modifications were however suggested in the way of attributing the  $S$  parameter, aimed at more realistically represent the age sequence of the oldest clusters, as well as those falling far from the mean  $S$  ridge line.

In our opinion, a revision of the age classification adopted by Persson et al. (1983) would also be worth, for

two reasons. First of all, the age calibration of SWB groups is based on old data, of very low quality if compared to those available nowadays. Second, the SWB classification, as well the behaviour of integrated *uvgr* colours, has never been analysed with the aid of SSP models of different ages, metallicities, and number of stars. In other words, it has not been demonstrated that the distribution of clusters in the  $Q_{ugr} \times Q_{vgr}$  diagram provides a good-quality age indicator. At least one of the assumptions of Persson et al. (1983), that the scattering along the ridge line is due only to observational errors, can be questioned by means of very simple simulations of star clusters. In fact, the stochastic dispersion of LMC cluster properties is not negligible in the visual colours, and more importantly, it occurs along preferential directions in colour-colour diagrams (see the analysis of Girardi et al. 1995 for *UBV*). It represents a potential origin of both uncertainties and systematic errors in the methods for age attribution based on colour-colour diagrams.

Table 3 presents the value of the  $S$  and  $t_{\text{PACFM}}$  age indicators, for those LMC clusters for which the *JHK* photometry is available. In the first column we have the parameter  $S$  as defined by Girardi et al. (1995) and according to the *UBV* data from Bica et al. (1996). It follows in the second column, the  $S$  as defined originally by Elson & Fall (1985),  $S_{\text{EF}}$ . We can notice that both values are very similar, since the listed clusters are in general bright ones, falling close to the ridge  $S$  line drawn in both works. We recall that the  $S$  parameter is shown to correlate with age according to  $\log(t/\text{yr}) = 6.227 + 0.0733 S$ , giving a r.m.s. precision of 0.14 dex in the age determination of rich clusters (Girardi et al. 1995). However, according to the latter authors, it can not be used to date old clusters of low metallicity (those with SWB type VII in the Magellanic Clouds). Therefore, these are assumed to have 15 Gyr, or equivalently  $S = 54.5$ . The  $t_{\text{PACFM}}$  from Persson et al. (1983) is listed in the third column of Table 3. It is essentially a non-calibrated age parameter.

Figure 7 presents the relation between the parameters  $S$  and  $t_{\text{PACFM}}$ , as well as histograms of their values, for the clusters of Table 3. It is clear that the relation is not linear, and that the clusters tend to concentrate at certain values of age parameters. For instance,  $S$  values around 23 and 38, and  $t_{\text{PACFM}}$  values around 150 are 220, are more frequent between the clusters. In Girardi et al. (1995), these peaks in the distribution of  $S$  are interpreted as being the signature of different episodes of enhanced cluster formation in the LMC. The histogram of  $t_{\text{PACFM}}$ , however, presents a peak around 190, and a minimum around 210, which have no counterparts in the distribution of  $S$ . This difference probably reflects the low number of objects in the sample. We notice also that  $t_{\text{PACFM}} = 200$  is exactly the transition value between clusters with  $V - K \simeq 1.5$  and 3 (see Fig. 2 in Persson et al. 1983, and Fig. 8 below). It corresponds, also, to a period of apparently fast evolution of  $B - V$  colours, according to the latter authors.

#### 4.2 The transition of $V - K$ colours

Figure 8 shows the age distribution of  $V - K$  colours of LMC star clusters, when we use the ages derived from the  $S$  parameter as in Girardi et al. (1995), or the age indicator

**Table 3.** Age indicators for LMC clusters with near-IR photometry.

Id. (NGC)	<i>S</i>	<i>S</i> <sub>EF</sub>	<i>t</i> <sub>PACFM</sub>	Id. (NGC)	<i>S</i>	<i>S</i> <sub>EF</sub>	<i>t</i> <sub>PACFM</sub>	Id. (NGC)	<i>S</i>	<i>S</i> <sub>EF</sub>	<i>t</i> <sub>PACFM</sub>
1466	–	49	274	1872	29	30	178	2108	36	36	–
1644	37	37	224	1898	–	50	–	2121	46	44	247
1711	21	20	122	1916	–	46	–	2134	28	28	193
1751	40	42	224	1943	24	25	150	2136	25	26	154
1755	24	24	142	1944	29	29	–	2154	38	39	229
1767	14	16	–	1951	25	24	–	2155	44	45	246
1774	22	23	113	1953	31	29	–	2156	28	26	–
1783	37	37	225	1978	41	45	239	2157	25	25	–
1786	–	48	–	1984	10	11	–	2159	24	25	–
1805	17	17	–	1986	23	24	135	2162	36	39	222
1806	38	40	231	1987	35	35	193	2164	24	23	160
1818	18	18	67	1994	13	15	–	2172	25	25	–
1831	32	31	211	2002	13	17	–	2173	41	42	233
1835	–	47	272	2004	12	15	11	2209	35	35	178
1841	–	42	292	2011	13	13	–	2210	–	48	277
1846	39	40	219	2019	–	46	265	2213	38	39	228
1850	23	21	–	2041	24	25	152	2214	23	22	140
1854	22	24	134	2058	25	26	162	2231	38	37	223
1855	22	22	–	2065	26	26	165	2257	–	51	285
1856	31	30	191	2070	18	14	–	H 11	–	51	283
1866	28	27	169	2100	16	17	50				
1868	33	33	–	2107	32	32	198				

Clusters with no *S* parameter are of SWB type VII, and then supposedly old ( $t \gtrsim 12$  Gyr).

*t*<sub>PACFM</sub>. We remark that there are many more clusters with ages determined by means of the former method.

In the upper panel we notice several interesting characteristics. First, for ages slightly larger than  $10^7$  yr, we have clusters with *V - K* colours spanning the range  $1 \lesssim (V - K) \lesssim 3$ . For those with *V - K* close to 3, the red colours can be explained by the presence of red supergiant (RSG) stars in clusters of similar age (see e.g. Arimoto & Bica 1989; Girardi & Bica 1993). Classical examples of these clusters are NGC 2004 and 2100 (see Bica, Alloin & Santos Jr. 1989). The youngest cluster in the sample (NGC 1834, with *S* = 10 and *V - K*  $\simeq$  1.2) is probably too young to contain red supergiant stars.

At ages around  $10^8$  yr, cluster colours concentrate around *V - K*  $\sim$  1.5, while at  $10^9$  yr they have *V - K*  $\sim$  3. The velocity of this colour transition, due to the high dispersion of the colours and to the small number of clusters, can not be precisely determined. However, comparison of the two panels in Fig. 8 reveals that the *S* age-ranking allows either for a fast colour transition at  $\simeq$  34, or for a *gradual* colour transition occurring in the interval  $30 < S < 40$ , while the *t*<sub>PACFM</sub> one would suggest (according to the interpretation originally given by Persson et al. 1983, see their Fig. 2), a fast colour transition occurring at *t*<sub>PACFM</sub> = 200.

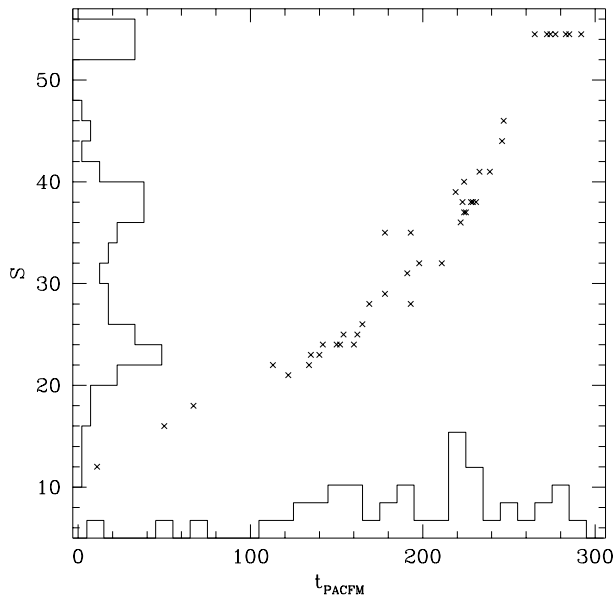
Therefore, the fast transition in *V - K* is not so clearly defined in the plot which uses the *S* parameter, which is arguably a better age indicator than *t*<sub>PACFM</sub>. We recall that the adoption of *t*<sub>PACFM</sub> as an age indicator allows also for a relatively fast transition of the *B - V* colours (see Fig. 3 in Persson et al. 1983) at almost the same age of the presumed *V - K* transition (see also Corsi et al. 1994). There is no sign of such a feature, however, in plots that relate the *S* parameter (and in turn of the *B - V* colour) with cluster

ages determined directly from the main-sequence turn-off magnitude (see Elson et al. 1988; and Fig. 11 in Girardi et al. 1995). Therefore, we point out that the fast transition of *V - K* at *t*<sub>PACFM</sub>  $\sim$  200, could simply reflect a deficiency of this parameter in representing the age sequence of star clusters, instead of a real feature of the *V - K* evolution.

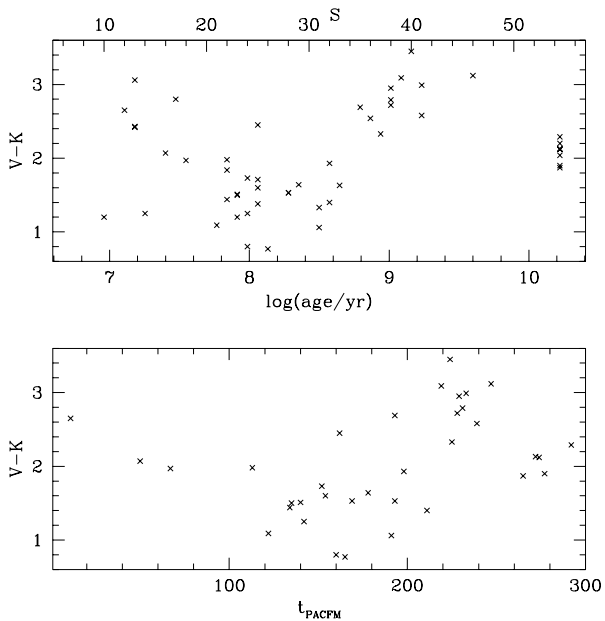
Finally, we notice that in the upper panel of Fig. 8, the old clusters (with assumed ages of 15 Gyr) have *V - K*  $\sim$  2, being bluer than those with  $\sim 10^9$  yr. This probably reflects their lower metallicity. According to Olzewski et al. (1991), the old clusters in the LMC have  $-1.5 > [\text{Fe}/\text{H}] > -2.2$ , in contrast with the young and intermediate-age ones, which have  $0.0 > [\text{Fe}/\text{H}] > -0.6$ .

Figure 9 presents the complete data for the *V - K*, *J - K*, and *H - K* colours, for ages derived from the *S* parameter. Superimposed, are the SSP models for *Z* = 0.008, and calculated with the Vassiliadis & Wood’s (1993) mass-loss rates (cf. Fig. 4). For  $\log(t/\text{yr}) < 7.8$ , we draw also the models of Bertelli et al. (1994) for *Z* = 0.02. The latter models are important for a discussion of the colours of clusters which contain RSG stars. We notice that models with *Z* = 0.02 reproduce well the location of the very young [ $\log(t/\text{yr}) < 7.8$ ] and red clusters. Those with *Z* = 0.008, instead, are too blue to describe most of the data in this age interval. This is probably related to the fact that theoretical models with *Z* = 0.008, in general, predict too blue RSGs with respect to those observed in LMC clusters. Other effects, as the sensitivity of the colours to the IMF slope (e.g. Girardi & Bica 1993), may also affect the colours in this age range around  $10^7$  yr.

With respect to the *J - K* and *H - K* colours, we recall that they refer only the form of the near-infrared spectrum. They are very sensitive to the presence of carbon stars in a



**Figure 7.** Relationship between the parameters  $S$  obtained by Girardi et al. (1995), and  $t_{\text{PACFM}}$  from Persson et al. (1983), for the LMC clusters of Table 3 which present both age indicators (crosses). The histograms along the two axes give the number distribution of both parameter. See the text for more details.



**Figure 8.** The time evolution of  $V - K$  for LMC clusters, according to two different age rankings: the  $S$  parameter as defined and calibrated by Girardi et al. (1995; upper panel), and the  $t_{\text{PACFM}}$  parameter from Persson et al. (1983; lower panel).

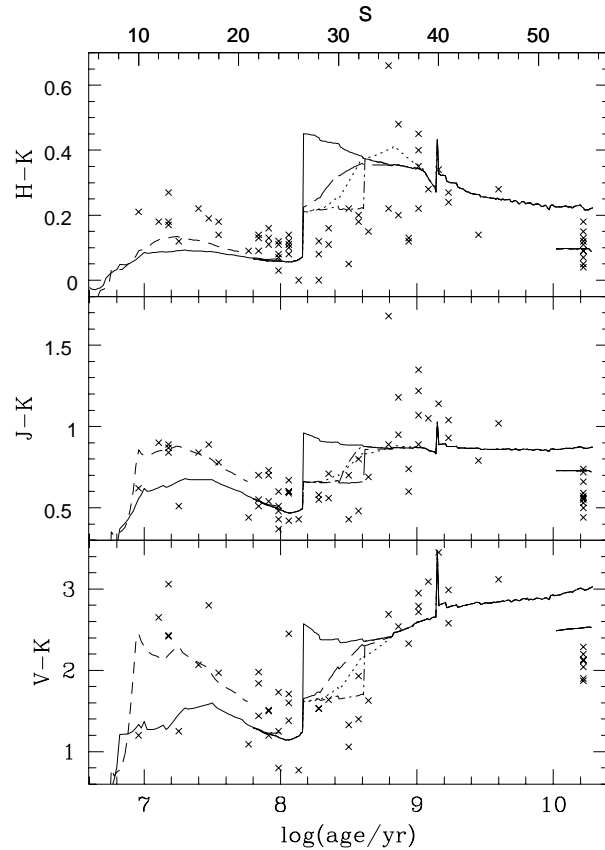


**Figure 9.** Data on the near-IR colours of LMC star clusters, compared to models of colour evolution with  $Z = 0.008$ , which assume the Vassiliadis & Wood (1993) prescription for the mass-loss rates. The meaning of the lines is as in Fig. 4. Models with  $Z = 0.001$  are shown only for  $t > 10$  Gyr. For  $\log(t/\text{yr}) < 7.8$  we present also the case  $Z = 0.02$  from Bertelli et al. (1994; short-dashed line).

stellar cluster (Persson et al. 1983; Frogel, Mould & Blanco 1990). The red  $J - K$  and  $H - K$  colours that occur in the clusters with age  $8.5 \lesssim \log(t/\text{yr}) \lesssim 9.2$ , in fact, can be attributed to the presence of carbon stars in this limited age range (see Frogel et al. 1990; Marigo et al. 1996b). As our models of SSPs do not differentiate M- and C-type AGB stars, they fail in giving a good description of these colours. This can be seen in the upper and middle panels of Fig. 9.

The lower panel, with the evolution of  $V - K$ , is far more illustrative. It shows that the  $Z = 0.008$  models for sufficiently young and old ages, reproduce the observed clumping of colours at values  $V - K \sim 1.5$  at  $10^8$  yr, and  $V - K \sim 3$  at  $10^9$  yr. The oldest models with  $Z = 0.001$  approximate to the colours  $V - K \sim 2$  observed for the oldest clusters. Anyway, this value of the metallicity is yet too high for allowing a significant comparison with the data for the old clusters (values of  $Z$  as low as 0.0005 would be required).

The most interesting comparison arises in the age range from  $10^8$  to  $10^9$  yr, in which the  $V - K$  colour transition takes place. We can see that models which assume no overlu-

minosity for the AGB stars (i.e., ‘classical’ models), present too red  $V - K$  colours in the first part of this age interval. Models which include this effect, instead, approximate to the mean locus of the observed points. Also the model which represents the prediction by Renzini (1992) – which assume a more dramatic prescription for the evolution of envelope burning stars, see Section 3.1 – would describe better the observed points than classical models. Unless the assumed prescriptions for the TP-AGB evolution are very far from the reality, *this can be seen as an indication for the occurrence of overluminosity (and hence envelope burning) in the AGB stars of the LMC with initial masses  $\gtrsim 3 M_{\odot}$ .*

### 4.3 The role of the RGB

Another point that we can observe in Fig. 9 is that the RGB appears in the SSP models at quite large ages [at  $\log(t/\text{yr}) = 9.08$ , or  $S = 39$ ], when the transition from  $V - K \sim 1.5$  to 3.0 is practically completed. Therefore, the development of the RGB has no role in this transition. The development of the AGB, instead, is determinant. This can be observed in the right panel of Fig. 3: were the TP-AGB absent in our models [as is practically the case when we use the Blöcker’s (1995) mass-loss rates], the transition of the  $V - K$  colour would also occur, but much more slowly. Values of  $V - K \simeq 3$  would be attained only at ages of  $\sim 10^{10}$  yr in this case, and not at  $\sim 10^9$  yr as observed.

This is not in contradiction with the results obtained from Corsi et al. (1994) and Ferraro et al. (1995), which conclude that the development of the AGB is the main responsible for the  $V - K$  transition. However, they suggest that the RGB appears in the Magellanic Cloud clusters with  $S > 35$ , i.e. practically in the age range in which the  $V - K$  colour more rapidly change (see Fig. 8), contrarily to our results. It is worth comparing our models with their data, in order to identify possible discrepancies.

These authors deal basically with two complementary data sets. Corsi et al. (1994) obtained  $BV$  CCD photometry for 11 LMC clusters with intermediate values of  $S$ . They determine quite precisely the location of the terminal main sequence ( $V_{\text{TO}}$ ) and the red clump of He-burning stars (or  $V_{\text{HB}}$ ) for each cluster. A plot of  $V_{\text{TO}}$  against  $V_{\text{HB}}$  (their Fig. 36, and Fig. 10 below) reveals clearly the presence of a minimum in the function  $V_{\text{HB}}(V_{\text{TO}})$ , for clusters around NGC 2209, which have  $S = 35$ . This minimum reflects the similar minimum in  $M_c^{\text{RGB}}(M_i)$  present in the stellar evolutionary models (Fig. 1), and should occur at ages immediately before the onset of the RGB. The two clusters observed in the plateau of the  $V_{\text{HB}}(V_{\text{TO}})$  curve, corresponding to clusters which have already well-developed RGBs, have  $S_{\text{EF}} = 39$  and 43 (Elson & Fall 1985), or  $S = 36$  and 41 (Girardi et al. 1995).

In Fig. 10 we present a similar plot of  $V_{\text{TO}}$  versus  $V_{\text{HB}}$ , comparing the Corsi et al. (1994) data with the results from our  $Z = 0.008$  models (continuous line). The latter are displayed in the diagram after shifted by a quantity corresponding to the mean apparent distance modulus of the LMC clusters,  $V - M_V = 18.7$ . These models seem to describe well the general distribution of points, especially in the minimum of the  $V_{\text{HB}}(V_{\text{TO}})$  curve. However, for the youngest clusters, the observed  $V_{\text{HB}}$  is systematically shifted to higher magnitudes with respect to the models. It is not easy to explain

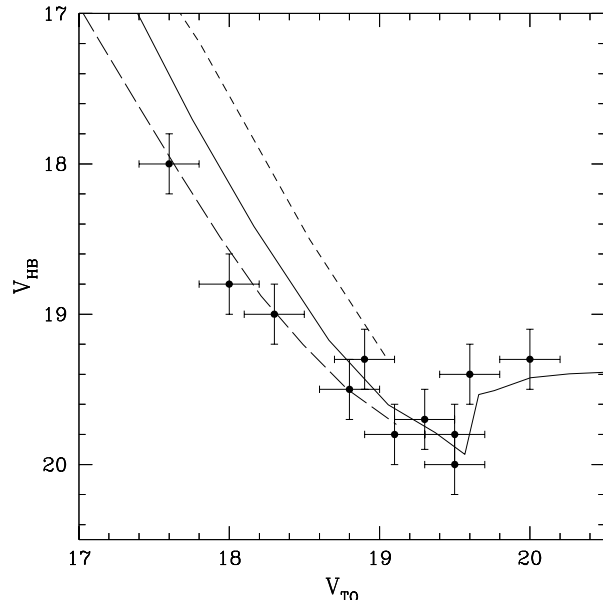


**Figure 10.** The magnitude of the clump of CHeB stars,  $V_{\text{HB}}$ , against the terminal-age main sequence,  $V_{\text{TO}}$ , as observed in LMC star clusters by Corsi et al. (1994; black dots) and as predicted by our  $Z = 0.008$  models (continuous line). The data are presented with the typical error bars of 0.2 mag in  $V$ . An apparent distance modulus of  $V - M_V = 18.7$  mag was assumed for the LMC. Long-dashed lines represent the models for  $Z = 0.02$  from Bertelli et al. (1994), for  $\log(t/\text{yr}) < 9$ , also computed with moderate convective overshoot. The short-dashed line presents the corresponding relation obtained from Alongi et al. (1993) models with  $Z = 0.008$ , but assuming the semiconvective scheme of mixing.

this shift. The adoption of a different distance modulus for the LMC, for instance, would change the situation only for those two clusters with  $V_{\text{TO}} > 19.5$ , the oldest in the sample.

Several factors could affect the relative  $V$  magnitude of TO and CHeB stars in the young clusters. Two of them are also illustrated in Fig. 10: (1) Models with higher metal and/or helium content tend to reproduce better the points with  $V_{\text{TO}} < 19$ , as shown by the Bertelli et al. (1994) models with  $[Z = 0.02, Y = 0.28]$  (long-dashed line in Fig. 10). (2) Models with more efficient convective overshoot also tend to present higher  $V_{\text{HB}}$  magnitudes for a given  $V_{\text{TO}}$ , (which would also lead to a better agreement with the data). This can be seen if we compare in Fig. 10 the models with  $[Z = 0.008, Y = 0.25]$  of Alongi et al. (1993) computed with the classical semiconvection scheme (short-dashed line), with our models obtained with the same chemical composition, but with the adoption of moderate convective overshoot (continuous line). Moreover, other effects as systematic errors in the bolometric corrections used to convert the theoretical quantities to the magnitude  $M_V$ ; or the blending or presence of double stars at the tip of the main sequence (see e.g. Maeder 1994), could also affect the quantities presented in Fig. 10. Given the complexity of factors in play, we limit ourselves to the comment that the figure points to a good agreement between theory and observations

in which concerns the behaviour of  $V_{\text{HB}}(V_{\text{TO}})$  curve in the vicinity of  $M_{\text{Hef}}$ .

Ferraro et al. (1995) have observed in *JHK* photometry a subsample of the clusters studied by Corsi et al. (1994). RGB stars were observed for clusters with  $S > 35$ , but unambiguously only in those with  $S > 37$ . They recognize that the present data, due to the problems of field contamination and small stellar statistics, should be improved in order to determine more precisely the age in which the RGB stars appear in the CMDs. Particularly unfortunate was the fact that the CMDs of the two clusters they observed in the range  $35 < S < 37$ , NGC 1987 and NGC 2108, can be severely contaminated by the LMC bar population.

Therefore, the  $S$  limit for the appearance of extended RGBs seems to be located somewhere between  $S = 35$  and  $39$ , being  $S = 37$  a more probable value. In our models, the RGB develops completely only at ages corresponding to  $S = 39$ . Is the difference between these two results significant? An answer to the above question would require a detailed revision of the adopted  $S$  vs.  $\log(\text{age})$  calibration, which is beyond the scope of this paper. Suffice it to say that systematic shifts in  $B - V$  colours, with respect to those observed in clusters, are possibly present in the models. These shifts probably amount to only  $\Delta(B - V) \simeq 0.1$  (corresponding to  $\Delta S \simeq 2$  in the age range here in consideration), and can be easily explained by the presence of inadequacies in the theoretical colour- $T_{\text{eff}}$  relations we used. Moreover, we recall that the relationship between the  $S$  parameter and age can be affected by a particularly insidious problem in the interval  $30 \lesssim S \lesssim 36$ : in this age range the intrinsic dispersion of cluster colours runs almost parallel to the  $S$  sequence in the  $(U - B)$  vs.  $(B - V)$  diagram (cf. Girardi et al. 1995). This determines a higher uncertainty in the ages of clusters found around this region of  $S$  parameter. It also suggests that, in future analysis of the subject, ages determined directly from main sequence photometry (or simply the  $V_{\text{TO}}$  quantity) should be preferred in order to provide an age ranking to the clusters.

We conclude that there is no fundamental contradiction between the conclusions obtained in this paper, and those from Corsi et al. (1994) and Ferraro et al. (1995). Both theory and observation can probably be improved in order to obtain a better agreement about the age of the onset of the RGB, but anyway the present disagreement, if any, is of modest amount.

We would like to stress also the necessity of more data concerning the Magellanic Cloud clusters, in order to provide conclusive checks to the current SSP models, in the age ranges they can be more uncertain. It includes obviously the age range from  $10^8$  to  $10^9$  yr, in which the main  $V - K$  transition occurs. Projects as those pursued by Corsi et al. (1994) and Ferraro et al. (1995) should certainly continue, in order to provide data for more clusters, so reducing the uncertainties related to the statistics of the giants stars. Moreover, the question of field contamination in the observed CMDs has revealed to be crucial in the observational studies carried out so far.

## 5 FINAL COMMENTS

This work shows that the colour (and hence spectral) evolution of the SSPs that contain AGB stars, is not as well established as generally supposed. Uncertainties in the theory of AGB evolution, regarding the dependency of mass loss rates on stellar parameters, and the effect of overluminosity with respect to the core mass–luminosity relation, are able to significantly modify the results obtained so far for SSPs with ages from about  $10^8$  to  $\sim 10^9$  yr. Also, the present models allow for a revision of the colour changes that follow the AGB and RGB developments. On the one hand, we argue that the colour transition due to the AGB development should be more gradual than classically predicted, thanks to the effect of AGB overluminosity. On the other hand, we confirm earlier suggestions that the RGB development does not cause a transition to redder colours, but indicate that a transient red phase should occur due to the reduction of the core-He burning lifetimes that accompanies the RGB development. The latter effect, however, probably does not produce significant observational counterparts.

The effect of overluminosity in the most massive AGB stars should be properly included in SSP calculations, in order to define precisely how the colour evolution occurs for different metallicities. This overluminosity is expected to affect the near-infrared colours of near-solar SSPs, and most colours of low-metallicity SSPs, for ages between  $\sim 10^8$  and  $\sim 3 \times 10^8$  yr. In fact, we show that the overluminosity provides a reasonable description for the observed colour evolution of  $V - K$  colours, from values  $\sim 1.5$  to  $3$ , in LMC clusters of these ages. We notice also that envelope burning (and overluminosity) in TP-AGB stars is thought to be particularly efficient at low-metallicities. Therefore, this effect is potentially important in describing the colour evolution of young low-metallicity stellar populations, even at visual pass-bands. All these aspects may be significant in view of realistically predicting the colour evolution of low-metallicity and young galaxies, observed at high redshifts.

## ACKNOWLEDGMENTS

L. Girardi acknowledges the constructive interaction with E. Bica, A. Bressan, C. Chiosi, P. Marigo, and E. Nasi, during the last few years, which made possible the development of this work. Thanks are due to A. Schmidt and M.V. Copetti for their efforts in providing him with suitable working conditions during a preliminary stage of this research; to the Department of Astronomy of the Padova University, and the Instituto de Física da Universidade Federal do Rio Grande do Sul for the repeated hospitality; and to the Alexander von Humboldt Foundation for financial support. A. Weiss and M. Groenewegen are acknowledged for the critical reading of the manuscript.

## REFERENCES

- Alexander D.R., Ferguson J.W., 1994, ApJ 437, 879
- Alongi M., Chiosi C., 1989, in *Astrophysical Ages and Dating Methods*, eds. E. Vangioni-Flam et al., Editions Frontières: Gif sur Yvette, p. 207

- Alongi M., Bertelli G., Bressan A., Chiosi C., Fagotto F., Greggio L., Nasi E., 1993, *A&AS* 97, 851
- Arimoto N., Bica E., 1989, *A&A* 222, 89
- Barbaro G., Bertelli G., 1977, *A&A* 54, 243
- Barbaro G., Olivi F.M., 1991, *AJ* 101, 922
- Battinelli P., Capuzzo-Dolcetta R., 1989, *ApJ* 347, 794
- Bertelli G., Bressan A., Chiosi C., Fagotto F., Nasi E., 1994, *A&AS*, 106, 275
- Bessell M.S., Brett J.M., 1988, *PASP* 100, 1134
- Bica E., Alloin D., Santos Jr. J.F.C., 1989, *A&A* 235, 103
- Bica E., Clariá J.J., Dottori H., Santos Jr. J.F.C., Piatti A., 1991, *ApJ* 381, L51
- Bica E., Clariá J.J., Dottori H., Santos Jr. J.F.C., Piatti A., 1996, *ApJS* 102, 57
- Blöcker T., 1995, *A&A*, 297, 727
- Blöcker T., Schönberner D., 1991, *A&A*, 244, L43
- Boothroyd A.I., Sackmann I.J., 1988, *ApJ* 328, 671
- Boothroyd A.I., Sackmann I.J., 1992, *ApJ* 393, L21
- Boothroyd A.I., Sackmann I.J., Ahern S.C., 1993, *ApJ* 416, 762
- Bowen G.H., 1988, *ApJ* 329, 844
- Bowen G.H., Willson L.A., 1991, *ApJ*, 375, L53
- Bressan A., Fagotto F., Bertelli G., Chiosi C., 1994a, *A&AS* 100, 647
- Bressan A., Chiosi C., Fagotto F., 1994b, *ApJS* 94, 63
- Bruzual A.G., Charlot S., 1993, *ApJ* 405, 538
- Charlot S., Bruzual G., 1991, *ApJ*, 367, 126
- Charlot S., Worthey G., Bressan A., 1996, *ApJ* 457, 625
- Chiosi C., Bertelli G., Bressan A., 1988, *A&A* 196, 84
- Chiosi C., Bertelli G., Bressan A., 1992, *ARA&A* 30, 305
- Corsi C.E., Buonanno R., Fusi Pecci F., Ferraro F.R., Testa V., Greggio L., 1994, *MNRAS* 271, 385
- Elson R.A.W., Fall S.M., 1985, *ApJ* 299, 211
- Elson R.A.W., Fall S.M., 1988, *AJ* 96, 1383
- Fagotto F., Bressan A., Bertelli G., Chiosi C., 1994a, *A&AS* 104, 365
- Fagotto F., Bressan A., Bertelli G., Chiosi C., 1994b, *A&AS* 105, 29
- Ferraro F.R., Fusi-Pecchi F., Testa V., Greggio L., Corsi C.E., Buonanno R., Terndrup D.M., Zinnecker H., 1995, *MNRAS* 272, 391
- Frogel J.A., Mould J., Blanco V.M., 1990, *ApJ*, 352, 96
- Girardi L., Bica E., 1993, *A&A*, 274, 279
- Girardi L., Chiosi C., Bertelli G., Bressan A., 1995, *A&A*, 298, 87
- Girardi L., Bressan A., Chiosi C., Bertelli G., Nasi E., 1996, *A&AS* 117, 113
- Groenewegen M.A.T., de Jong T., 1993, *A&A*, 267, 410
- Herwig F., 1996, in *Stellar Evolution: What Should Be Done*, 32nd Liège Int. Astrophys. Coll., eds. A. Noels et al., p. 441.
- Iben Jr. I., Truran J.W., 1978, *ApJ* 220, 980
- Iben Jr. I., Renzini A., 1983, *ARA&A* 21, 271
- Iglesias C.A., Rogers F.J., 1996, *ApJ* 464, 943
- Jeffries R.D., 1997, *MNRAS* 288, 585
- Kurucz R.L., 1992, in *The Stellar Populations of Galaxies*, eds. B. Barbuy and A. Renzini, Dordrecht: Kluwer, p. 225
- Lançon A., Rocca-Volmerange B., 1992, *A&AS* 96, 593
- Lançon A., Rocca-Volmerange B., 1996, *New Astron.* 1, 215
- Maeder A., 1974, *A&A* 32, 177
- Marigo P., Bressan A., Chiosi C., 1996a, *A&A*, 313, 545
- Marigo P., Girardi L., Chiosi C., 1996b, *A&A*, 136, L1
- Marigo P., Bressan A., Chiosi C., 1998, *A&A* 331, 564
- Matteucci F., Tornambè A., 1985, *A&A* 142, 13
- Mihalas D., Hummer D.G., Mihalas B.W., Däppen W., 1990, *ApJ* 350, 300
- Olszewski E.W., Schommer R.A., Suntzeff N.B., Harris H.C., 1991, *AJ* 101, 515
- Persson S.E., Aaronson M., Cohen J.G., Frogel J.A., Matthews K., 1983, *ApJ*, 266, 105
- Racine R., 1973, *AJ* 78, 180
- Reimers D., 1975, *Mem. Soc. R. Sci. Liège*, ser. 6, vol. 8, p. 369
- Renzini A., Voli M., 1981, *A&A* 94, 175
- Renzini A., Buzzoni A., 1986, in *Spectral Evolution of Galaxies*, eds. C. Chiosi and A. Renzini, Dordrecht: Reidel, p. 195
- Renzini A., 1992, in *The Stellar Populations of Galaxies*, eds. B. Barbuy and A. Renzini, Dordrecht: Kluwer, p. 325
- Rocca-Volmerange B., 1996, in *From stars to galaxies: the impact of stellar physics on galaxy evolution*, ASP Conf. Ser. 98, eds. C. Leitherer et al., p. 567
- Sackmann I.J., Boothroyd A.I., 1991, *ApJ* 366, 529
- Santos Jr. J.F.C., Frogel J.A., 1997, *ApJ* 479, 764
- Schönberner D., 1981, *A&A* 103, 119
- Searle L., Wilkinson A., Bagnuolo W.G., 1980, *ApJ* 239, 803
- Sweigart A.V., Greggio L., Renzini A., 1990, *ApJ* 364, 527
- Terndrup D.M., Frogel J.A., Withford A.E., 1991, *ApJ* 378, 742
- Tinsley B.M., 1980, *Fundam. of Cosmic Phys.* 5, 287
- Tuchman Y., Glasner A., Barkat Z., 1983, *ApJ* 268, 356
- van den Bergh S., 1981, *A&AS* 46, 79
- Vassiliadis E., Wood P.R., 1993, *ApJ*, 413, 641
- Wagenhuber J., 1996, PhD thesis, Technisch Universität München
- Wagenhuber J., Groenewegen M., 1997, *A&A*, submitted.
- Weiss A., Peletier R.F., Matteucci F., 1995, *A&A* 296, 73
- Worthey G., 1994, *ApJS*, 95, 107